Open Journal of Inorganic Chemistry, 2016, 6, 89-113
Published Online April 2016 in SciRes. http://www.scirp.org/journal/ojic
http://dx.doi.org/10.4236/ojic.2016.62006

Spectral, Thermal and Antibacterial Studies for Bivalent Metal Complexes of Oxalyl, Malonyl and Succinyl-bis-4-phenylthiosemicarbazide Ligands

Ragab R. Amin[1*], Ahmed A. M. El-Reedy[2], Tajedin Y. Alansi[3], Yamany B. Yamany[4]

[1]Basic Science Department, Faculty of Engineering, Nahda University, Beni-Suef, Egypt
[2]Basic and Applied Science Department, Faculty of Oral and Dental Medicine, Nahda University, Beni-Suef, Egypt
[3]Chemistry Department, Adama Science and Technology University, Adama, Ethiopia
[4]Pharmaceutical Chemistry Department, Faculty of Pharmacy, Taif University, Taif, Saudia Arabia
Email: *rramin2010@.yahoo.com, Ahmed.reedy78@gmail.com

Received 16 November 2015; accepted 19 February 2016; published 22 February 2016

Abstract

The thermogravimetry (TG) and derivative thermogravimetry (DTG) have been used to study the thermal decomposition of some oxalyl (H_4OxTSC), malonyl (H_4MaTSC) and succinyl-bis-4-phenyl-thiosemicarbazide (H_4SuTSC) ligands and their metal complexes using Horowitz-Metzger (HM) and Coats-Redfern methods. The kinetic thermodynamic parameters such as: E*, ΔH*, ΔS*and ΔG* are calculated from the DTG curves. The isolated complexes have the general composition $[M_2(L)(H_2O)_6]$, where M=Cu(II), Zn(II), L=MaTSC and M=Co(II), Cu(II) or Sn(II) and L=Su TSC and $[M_2(L)(H_2O)_n]\cdot nH_2O$ where M=Cu(II), Co(II) or Sn(II), L=OxTS or Ma TSC. The tested compounds show a good activity against four strains of bacteria Gram negative *Escherichia coli*, *Pseudomonas aeruginosa* species and gram-positive *Bacillus cereus* and *Staphylococcus aureus*.

Keywords

Metal (II) Complexes, Bis-Thiosemicarbazide, Thermogravimetric, Antibacterial Studies

1. Introduction

Thiosemicarbazide and its derivatives have received considerable attention because of their pharamacological

*Corresponding author.

How to cite this paper: Amin, R.R., El-Reedy, A.A.M., Alansi, T.Y. and Yamany, Y.B. (2016) Spectral, Thermal and Antibacterial Studies for Bivalent Metal Complexes of Oxalyl, Malonyl and Succinyl-bis-4-phenylthiosemicarbazide Ligands. *Open Journal of Inorganic Chemistry*, **6**, 89-113. http://dx.doi.org/10.4236/ojic.2016.62006

properties [1]. Thiosemicarbazide complexes show a broad spectrum of anticancer activity [2] [3]. Also, thiosemicarbazide derivatives are of current interest with respect to their uses as analytical reagents for separations of metal(II) ions [4]-[7], analytical determination of metal ions [8] [9], and clinical analysis [10]. Most of these compounds have antifungal [11]-[12], antimicrobial [13] and antitumor activity [14]-[16], as well as radiopharmaceuticals applications [17]. Continuing our studies for the chemical and electrochemical synthesis of new metal complexes of ligands containing N, S and O atoms through the reaction of metal ions scarified from the anodic dissolution of metals [18] [19]. Our aim work in this paper to report novel complexes prepared from the reaction between bisthiosemicarbazi decompounds which have a good ability to form chelate complexes with transition metal [18]-[20]. We report here the thermal, spectral and biological evaluations of Co(II), Cu(II), Zn(II) and Sn(II) complexes for 1,1-oxalyl, malonyl and succinyl-bis-4-phenylthiosemicarbazide ligands. The modern spectroscopic investigations are used to elucidate the structure of the prepared materials. The thermal decomposition is also used to infer the structure of the metal complexes and to calculate the different thermodynamic activation parameters.

2. Experimental

2.1. The Organic Compounds

1) ***Preparation of* 1,1-*Oxalylhydrazide*:** 1,1-oxalyldihydrazine was prepared by adding oxalyl chloride (7 gm, 0.05 mol) to alcoholic solution of hydrazine hydrate (5 gm, 0.1 mole). The reaction mixture was exothermic and left to cool with stirring. A white crystal precipitate was formed and washed with ethanol diethyl ether and left to dry.

2) ***Preparation of* 1,1-*Oxalylbis* (4-*phenylthiosemicarbazide*):** It was prepared by adding phenylisothiocynate (2.8 gm, 0.02 mol) to an alcoholic solution of oxalic acid dihydrazide (1.18 gm, 0.01 mole). The reaction mixture was refluxed for 1 hour and left to cool with stirring. The resulting white crystals were collected and washed with ethanol and diethyl ether, respectively. The resulting solids were filtered hot, washed with hot dist. water, EtOH and dried by Et_2O and finally dried in vacuum over silica gel (**Figure 1**).

3) ***Preparation of* 1,1-*Malonylbis-phenylthiosemicarbazide*:** 1,1-Malonyl bis-4-phenylthiosemicarbazide) was prepared by adding phenylisothiocynate (1.8 gm, 0.02 mol) to an alcoholic solution of malonic acid dihydrazide (1.32 gm ≈ 0.01 mole). The reaction mixture was refluxed for 1 hour and left to cool with stirring. The resulting white crystals were collected and washed with ethanol and diethyl ether, respectively. The resulting solids were filtered hot, washed with hot dist. water, EtOH and dried by Et_2O and finally dried in vacuo over silica gel.

4) ***Preparation of* 1,1-*Succinylbis*-4-*phenylthiosemicarbazide*:** It was prepared by the same way [20]-[21].

2.2. The In-Organic Compounds

The preparative results show that the direct electrochemical oxidation of the metals in the presence of a ligand solution is a one-step process and represents a convenient and simple route to a variety of transition metal complexes. The apparatus used in the electrochemical reaction consists of a tall-form 100 mL Pyrex beaker containing 50 mL of the appropriate amount of the organic ligand dissolved in acetone solution. The cathode is a platinum wire of approximately 1 mm diameter. In most cases, the metal (2 - 5 g) was suspended and supported on a platinum wire. Measurements of the electrochemical efficiency, Ef, defined as moles of metal dissolved per Faraday of electricity, for the M/L system (where L = ligand used) gave $E_f = 0.5 \pm 0.05$ mol·F^{-1}.

2.3. Synthesis of Metals Complexes

Electrolysis of cobalt metal into 60 ml of anhydrous acetone solution of 1,1-oxalaylbis (4-phenylthiosemi-carbazide)ligand as an example, (1.2 gm, 5 mmol), 0.5 mg Et_4NClO_4 dissolved in two drops of water and 20 V current led to dissolution of 116 mg of Co during 120 min. (E_f = 0.5 mol·F^{-1}). Since, most of the products are insoluble in the reaction mixture, the collection procedure involved filtration, after which the solid was washed with diethyl ether. The resulting green powder was collected. By the same way Cu, Zn, and Sn complexes were isolated and all the data for carbon, hydrogen and nitrogen were gathered in **Table 1**.

3. Spectral, Analytical and Physical Measurements

3.1. IR, Raman and 1H-NMR Spectra

Infrared spectra for the three ligands and their metal complexes were recorded by Perkin Elmer FTIR 1605 using

KBr pellets (**Figures S1-S3**). Also, Raman spectra for the ligands, Zinc(II) and Sn(II) metal complexes were recorded in the solid state on Thero Nicolet FT-Raman (USA) with a wavelength 1064 nm power according sample resolution was 8 cm^{-1} at National Research Center, Cairo, Egypt (**Figures S4-S6**). The ^{1}H NMR spectra were recorded on an Varian Mercury VX-300 NMR spectrometer. ^{1}H-NMR spectra were run at 300 MHz and ^{13}C-NMRspectra were run at 75.46 MHz in deuterated dimethylsulphoxide (DMSO-d_6).

3.2. Electronic and Mass Spectra

The electronic spectra for all the ligands and the metal complexes solutions were measured in UV/Vis range (190 - 1100) nm using Helios UV Spectrometer at Center Photo energy, Ain-Shams University. Mass spectra were recorded at SHIMADZU GC MS-QP 1000 EX Micro analytical Center, Cairo Universal, Giza and Al-Azher University, Egypt (**Figures S7-S9**).

3.3. Magnetic Molar Conductance Measurements

Magnetic measurements were carried out on a Sherwood scientific magnetic balance using Gouy method. Molar conductivities of freshly prepared 1.0×10^{-3} $mol \cdot L^{-1}$ DMSO solutions were measured using Jenway 4010 conductivity meter.

3.4. Microanalytical and Magnetic Measurements

Carbon and hydrogen contents were determined using a Perkin-Elmer CHN 2400 analyser. Magnetic measurements were carried out on a Sherwood scientific magnetic balance using Gouy method.

Table 1. Significant IR spectral bands (cm^{-1}) of the ligand of 1,1-oxalyl-, malonyl, succinylbis-4-phenylthiosemicarbazide and their metal complexes.

Assignments	The compounds														
	(I)	(Ia)	(Ib)	(Ic)	(Id)	(II)	(IIa)	(IIb)	(IIc)	(IId)	(III)	(IIIa)	(IIIb)	(IIIc)	(IIId)
υ(OH)	----	3458	3447	3460	----	----	3407	3435	3429	3429	----	3466	3396	3447	3392
$\upsilon(N^4H)$	3306	3234	3230	3211	3300	3310	3237	3238	3305	3305	3310	3237	3238	3305	3305
$\upsilon(N^2H)$	3196	3181	3175	3174	3198	3196	3179	3180	3194	3197	3196	3220	3202	3200	3198
υ(NH)	3092	3111	3109	3100	3109	3111	3109	3111	3105	3111	3107	3115	3115	3109	3115
CH-arom.	3064	3055	3030	3046	3000	3005	3034	3053	3005	3007	3005	3032	3039	3001	3007
CH-aliph.	2940	2932	2941	2940	2940	2940	2980	2934	2938	2940	2940	2943	2938	2938	2940
υ(C=O)/υ(NCO)	1651	1595	1601	1593	1595	1657	1595	1599	1591	1599	1670	1595	1597	1595	1599
Thioamide I [β(NH)/υ(CN)]	1402	1422	1443	1425	1435	1400	1420	1431	1416	1440	1400	1418	1450	1418	1445
Thioamide II [υ(CN)/β(NH)]	1342	1398	1375	1362	1398	1341	1400	1400	1400	1400	1341	1368	1379	1377	1400
δ(OH)	----	1307	1306	1308	1308	----	1306	1310	1310	1308	----	1307	1319	1310	1308
υ(C-O)	----	1292	1287	1287	1246	----	1290	1219	1273	1246	----	1245	1232	1246	1246
υ(N–N)	902	934	941	924	924	902	935	945	924	925	923	975	960	966	964
υ(C=S)/υ(C-S)	831	755	756	777	775	814	743	772	777	777	827	755	775	777	773
υ(M-O)	-----	505	500	495	490	-----	493	501	490	490	-----	500	490	492	495
υ(M-N)	-----	415	420	415	417	-----	421	428	418	421	-----	415	425	421	415

3.5. Thermal Investigation

Thermogravimetric analysis (TGA and DTG) were carried out in dynamic nitrogen atmosphere (30 ml/min) with a heating rate of 10˚C/min using a SchimadzuTGA-50H thermal analyzer (**Figures S10-S12**).

3.6. Antibacterial Investigation

Bacterial cultures and growth conditions: Gram negative *Escherichia coli*, *Pseudomonas aeruginosa* species and gram-positive *Bacillus cereus*, *Staphylococcus aureus* species and fungal *Aspergillus fumingatus*, Candidaalbicans were used as test microorganisms. The surface of the medium was inoculated and covered with the tested organisms. The agar surface was allowed to dry from 3 to 5 minutes before applying disks. The disks were dipped into a beaker of the chemicals using sterile forceps and placed them in the previous medium. Cultures plates of bacteria were incubated for grown at 37˚C for 48 hours. Chloramphenicol was used as a standard antibacterial agent and Terbinafin was used as a standard antifungal agent.

4. Results and Discussion

4.1. Infrared Spectra of H_4OxTSC (I) and Its Metal Complexes

The IR spectrum of compound **I** shows bands at 3306, 3196, and 3092 cm^{-1} for the free-NH groups present in the ligand. The bands occurring at 1651, 1402, 1342, 902 and 831 cm^{-1} are assigned to ν(C=O), thioamide I [β(NH) + ν(CN)], thioamide II [ν(CN) + β(NH)], ν(N-N) and ν(C=S), respectively [22]-[27]. The assignments of the infrared bands, **Table 1**, were performed by comparing the spectra of the complexes with the free ligands. The bands due to ν(C=S) and ν(C=N) groups appeared at 802 and 1533 cm^{-1}. On complexation, the bands of the thiosemicarbazide moiety respect to ν(C=S) and ν(C=N) are shifted towards higher wave numbers and notice that the very strong peak of ν(C=S) may be disappeared or decreasing in its intensity. The bands due to ν(C=S), ν(N–N) and ν(C=N) groups appeared at 835, 1101 and 1602 cm^{-1} (**Figure 1**).

The IR spectra of Copper complex **Ia** compared with ligand H_4OxTS, indicates that bands due to ν(NH), ν(C=O) and ν(C=S) are absent, but new bands appear at ca. 1651 and 831 cm^{-1} due to ν(N=C) and ν(C-S), respectively, suggesting removal of both the hydrazinic protons via enolisation and thioenolisation and bonding of the resulting enolic oxygen and thiolato sulfur takes place with Co(II), Cu(II), Zn(II) and Sn(II). Furthermore, the ligand bands due to thioamide I, thioamide II and ν(N-N) undergo a positive shift of in the range (20 - 41 cm^{-1}), (20 - 56 cm^{-1}) and (22 - 39 cm^{-1}) respectively. Some new appear bands in the range (755 - 777cm^{-1}) assigned to groups (C-S) vibrations. This is also confirmed by the appearance of bands in the range of 395 - 417 cm^{-1}, this has been assigned to the ν(M–N) [28], and the appearance of bands in the range of 490 - 505 cm^{-1}, this has been assigned to the ν(M–O). A strong band found at 902 cm^{-1} is due to the ν(N–N) group of the 1,1-oxalylbis(4-phenyl-thiosemicarbazide. Thus the ligand behaves as tridentate chelating agent coordinating through azomethine nitrogen, thiolate sulphur andenolic oxygen (**Figure 2**, **Figure 3**).

4.2. Raman Spectra

The Raman spectrum shows bands at 3201 cm^{-1} for the NH groups present in H_4MaTS ligand. The bands occurring at 1635, 1405, 1355, 1088 and 824 cm^{-1} are assigned to ν(C=O), thioamide I [β(NH) + ν(CN)], thioamide II [ν(CN) + β(NH)], ν(N-N) and ν(C=S), respectively [29]-[32] (**Figure 4**). An exhaustive comparison of the Raman spectra of the ligand and complexes gave information about the mode of bonding of the ligand in metal

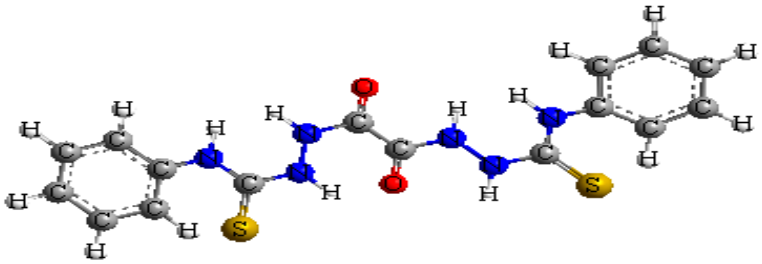

Figure 1. 1,1-Oxalyl-bis(4-phenylthiosemicarbazide) H_4OxTSC (I).

Ph-NH-CS-NH-NH-CO-CO-NH-NH-CS-NH-Ph.

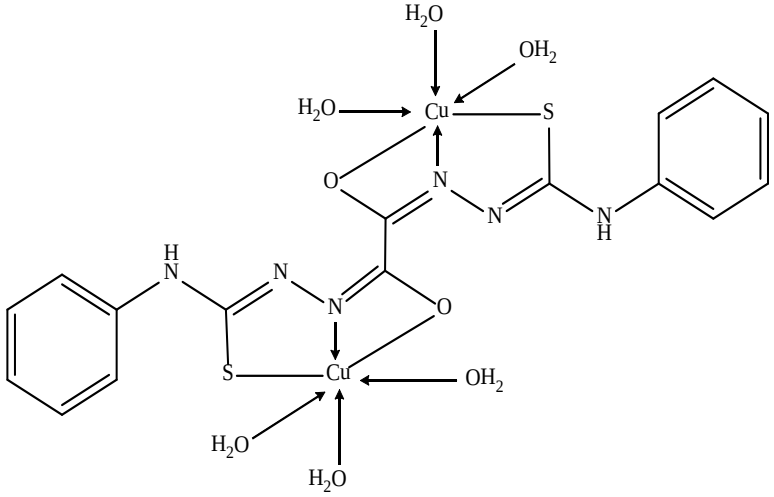

Figure 2. 1,1-Oxalaylbis(4-phenylthiosemicarbazide) bis-copper trihydrate (**Ia**).

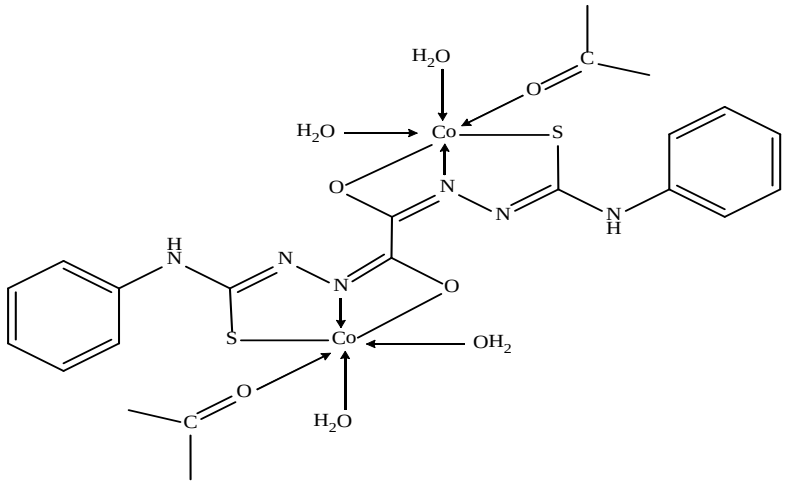

Figure 3. 1,1-Oxalaylbis-4-phenylthiosemicarbazide distorted octahedral cobalt monoacetonedihydrate (**Ib**).

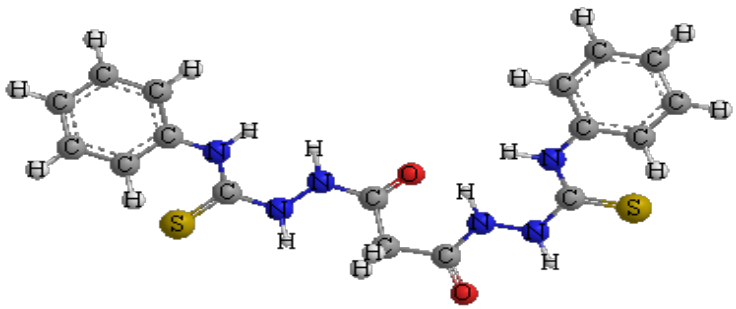

Figure 4. 1,1-Malonyl-bis(4-phenylthiosemicarbazide) H_4MaTSC (II). Ph-NH-CS-NH-NH-CO-CH_2-CO-NH-NH-CS-NH-Ph.

complexes. The Raman spectrum of complexes [Zn_2(MaTS)(H_2O)$_6$]) when compared with [H_4MaTS], indicates that bands due to ν(NH), ν(C=O) and ν(C=S) are absent, but new bands appear at ca. 1593 and 779 cm^{-1} due to ν(N=C) and ν(C-S), respectively, suggesting removal of both the hydrazinic protons via enolisation and thi-

oenolisation and bonding of the resulting enolic oxygen and thiolato sulfur takes place with Zn(II). Furthermore, the ligand bands due to thioamide I, thioamide II and ν(N-N) undergo a positive shift of (39 cm^{-1}), (40 cm^{-1}) and (2 cm^{-1}) respectively. Ramanbands of complexes are appear of bands at (779 cm^{-1}) assigned to groups (C-S) vibrations. It indicates that thione sulphur and also the enolic oxygen coordinates to the metal ion [33]-[35]. Thus, it may be concluded that the ligand behaves as hexadentate chelating agent coordinating through azomethine nitrogen and thiolate sulphur. The Raman spectrum of [H_4SuTS] shows bands at 3201, 3095 and 3063 cm^{-1} for the two-NH groups present in the ligand. The bands occurring at 1650, 1405, 1355, 900 and 824 cm^{-1} are assigned to ν(C=O), thioamide I [β(NH) + ν(CN)], thioamide II [ν(CN) + β(NH)], ν(N-N) and ν(C=S), respectively [33]-[35]. Raman spectral data of all the ligands and the metal complexes are summarized in **Table 2**.

4.3. Electronic Spectra

The electronic spectrum of $[Cu_2(OxTS)(H_2O)_6]\cdot 3H_2O$, **Ia**, has bands characteristic for an octahedral geometry [35]. The spectrum shows (**Table 3**) two bands at 20,600 and 31,950 cm^{-1} assigned to the $^4T_1g \rightarrow {}^4A_2g$ (ν_2) and $^4T_1g \rightarrow {}^4T_1g$ (P) (ν_3) transitions, respectively, in an octahedral structure. These bands were used to calculate the third spin-allowed band, $^4T_1g \rightarrow {}^4T_1g$ [20]. The other ligand field parameters, B, β and the ν_2/ν_1 values were calculated to be 1060 cm^{-1}, 1.2 and 2.2, respectively, and are in good agreement with those reported for octahedral Co(II) complexes. The electronic spectrum of $[Co(OxTS)(H_2O)_6]\cdot 6H_2O$, **Ib**, shows shoulder bands at 32,260 and 20,600 cm^{-1}. The observed bands are due to $^2B_1g \rightarrow {}^2Eg$ and $^2B_1g \rightarrow {}^2A_1g$ transitions, on the basis of octahedral geometry is suggested [35].

4.4. Magnetic Susceptibility

The observed values of magnetic moment for complexes are generally diagnostic of the coordination geometry about the metal ion. Co(II) has the electronic configuration $3d^*$ and should exhibit a magnetic moment higher than that expected for two unpaired electrons in octahedral (1.5 - 3.3 BM). The magnetic moment observed for the Co(II) complexes lies in the value of 3.2 BM which is consistent with the octahedral stereochemistry of the complexes. Room-temperature magnetic moment of the Cu(II) complexes lies in the range of 1.5 BM, corresponding to one unpaired electron.

4.5. ^{1}H-NMR Spectra

The ^{1}H-NMR spectra of compounds **Ic** and **IIc** on comparing with that of the ligands indicates that the ligands acts as a hex dentate through the nitrogen atom of C=N oxygen atom of C=O and sulfur atom of C=S. ^{1}H-NMR spectrum of zinc (II) complex is in agreement with the suggested coordination through the C=N and C=S groups by the presence of the signals of (two from 2NH amine groups and two protons from 2NH amide groups).

Table 2. Significant Raman spectra bands (cm^{-1}) of 1,1-oxalyl, malonyl, succinyl-bis(4-phenylthiosemicarbazide) and its metal complexes.

Assignments	The compounds							
	(I)	**(Ic)**	**(Id)**	**(II)**	**(IIc)**	**(III)**	**(IIIc)**	**(IIId)**
$\upsilon(N^4H)$	3307	----	----	3201	3209	3201	3260	3300
$\upsilon(N^2H)$	3199	3205	3205	3063	3062	3095	3135	3100
CH-arom.	3063	3062	3063	2934	2933	3063	3064	3063
CH-aliph.	2935	2931	2925	1635	1593	3005	3004	3005
υ(C=O)	1720	----	----	1405	1444	2934	2931	2925
υ(C=N)	1596	1594	1595	1355	1395	1650	1596	1593
υ(N–N)	1090	1091	1125	----	1315	1405	1439	1450
υ(C=S)	781	779	780	1088	1090	1355	1395	1390
υ(M-N)	-----	395	416	824	779	----	1319	1294

Table 3. The electronic spectral data of oxalyl, malonyl and succinyl-bis(4-phenylthiosemicarbazide) and its metal complexes.

Compounds	λ_{max} nm (cm^{-1})				
	π-π^*, C=S	**n-π^*, C=S**	**d-d transition**		
(I)	256, (39060)	314, (31850)	------	------	------
(Ia)	260, (38460)	313, (31950)	494, (20240)	559, (17889)	578, (17300)
(Ib)	268, (37300)	310, (32260)	486, (20600)	540, (18520)	------
(Ic)	265, (37740)	317, (31550)	------	------	------
(Id)	266, (37600)	324, (30860)	------	------	------
(II)	287, (34840)	344, (29070)	------	------	-----
(IIa)	288, (34720)	342, (29240)	462, (21650)	485, (20620)	522, (19160)
(IIb)	308, (32470)	358, (27930)	466, (21460)	493, (20280)	524, (19080)
(IIc)	284, (35210)	344, (29070)	------	------	-----
(IId)	288, (34720)	330, (30300)	------	------	-----
(III)	264, (37880)	328, (30490)	------	------	-----
(IIIa)	296, (33780)	356, (28090)	540, (18520)	600, (16670)	622, (16080)
(IIIb)	256, (39060)	320, (31250)	543, (18420)	610, (16390)	-----
(IIIc)	280, (35710)	332, (30120)	-----	-----	-----
(IIId)	260, (38460)	304, (32890)	-----	-----	-----

(H_4OxTS) ^{1}H-NMRδ (ppm): 9.75(N5, 17H amide group), 1.95(N6, 18H amine group), 3.6(CN9, 21H aromatic), 6.6 - 7.5(CH-aromatic).

[Zn_2(OxTS)(ac)$_2$]·2H_2O^{1}H-NMRδ (ppm): 1.19(CH_3 acetone), 2.7(H_2O) (NH amide groups disappeared), (NH amine groups disappeared), 3.5(9,21CNH aromatic), 6.6-7.5(CH-aromatic shifted).

(H_4SuTS)^{1}H-NMRδ (ppm): 9.7(7,19NH amide group), 1.95(8, 20NH amine group),4(11, 23CNH aromatic), 2.5(3, 4CH_2) 6.6 - 7.75(CH-aromatic).

[Zn_2(SuTS)(ac)$_2$]2(H_2O)^{1}H-NMRδ (ppm): 1.1(H_2O), 1.2(CH_3 acetone) (NH amide groups disappeared), (NH amine groups disappeared), 2.5(CH_2), 4(CNH aromatic), 6.6 - 7.75(CH-aromatic shifted).

4.6. Mass Spectrum

The electronic impact mass spectrum of the ligand **I** shows a molecular ion (M+) peak at *m*/*z* = 243 amu corresponding to species $C_9H_7N_3OS$, which confirms the proposed formula. It also shows series of peaks at 70, 88, 111, 127 and 170 amu corresponding to various fragments. The intensities of these peaks give the idea of the stabilities of the fragments. The electronic impact mass spectrum of the **Ia** complex 1,1-oxalayl-bis (phenylthiosemicarbazide) cobalt monoacetone dehydrate shows a molecular ion (M+) peak at *m*/*z* = 758 amu corresponding to species [$C_{22}H_{30}Co_2N_6O_8S_2$], which confirms the proposed formula. It also shows series of peaks at 39, 75, 90, 111, 127, 138, 169, 184, 201, 226, 243, 271 and 336 amu corresponding to various fragments.

5. Thermogravimetric Analysis

Thermogravimetric analysis curves (TGA and DTG) of **I**, **Ia**, **Ib and Ic** are discussed (**Tables 4-6**). Compound I was thermally decomposed in mainly decomposition steps within the temperature range 25˚C - 700˚C. The first step (obs. = 42.5%, calc. = 42.4%) at 25˚C - 237˚C, may be attributed to the liberation of the 2(N_2H_2), 2(HCNS) and 1/2O_2 fragments. The second step at 237˚C - 337˚C (obs. = 30.2%, calc. = 30.4%), is accounted for the removal of 1/2O_2 and C_4H_4.

The complex **Ia** was thermally decomposed in five successive decomposition steps within the temperature

range 25˚C - 1000˚C. The first step (obs. = 6%, calc. = 6.6%) at 25˚C - 175˚C, may be attributed to the liberation of the 3 water molecules. The second step at 175˚C - 390˚C (obs. = 29.2%, calc. = 28.6%), is accounted for the removal of 2 acetone, 4 water and N_3H_3 fragment. The decomposition third step at 390˚C - 707˚C (obs. = 18.3%, calc = 18.9%) is accounted for the removal of ($C_4N_3S_2$) fragment. The fourth step at 707˚C - 990˚C (obs. = 22.8%, calc = 22.8%) is accounted for the removal of (C_9H_7) fragment. The rest of the ligand molecule was removed and fifth the decomposition of the Co(II)/L complex molecule ended with a final 2CoO and residual carbon $3/2C_2$ fragment (obs. = 23.7%, calc = 22.9%).

The TG curve of **Ib** complex indicates that the mass change begins at 25˚C and continuous up to 1000˚C. The first and second mass loss corresponds to the liberation of the 12 water molecules and two (HCN) fragment (obs. = 34.4%, calc = 33.9%) at 25˚C - 342˚C. The third step occurs in the range 342˚C - 475˚C and corresponds to the loss of (CN_4S) (obs. = 12.8%, calc = 12.6%). The fourth and fifth decomposition step are final decomposition organic ligand to the $C_{13}H_8$, $1/2S_2$, O_2 fragments and Cu_2 metal residual atoms (obs. = 52.8%, calc = 53.4%).

Ic complex was thermally decomposed in mainly five decomposition steps within the temperature range 25˚C - 700˚C. The first decomposition step (obs. = 20.64%, calc = 20.64%) at 25˚C - 245˚C, may be attributed to the liberation of two water and two acetone molecules. The second step at 245˚C - 386˚C (obs. = 23.4%, calc = 23.6%) is accounted for the removal of the 2(HCN), $2N_2$ and S_2 fragments. The third step found within the temperature 386˚C - 700˚C (obs. = 19.7%, calc = 19.96%). The rest of the ligand molecule was removed and fourth the decomposition of theligand molecule ended with a final residue of (C_8H_4), (ZnO) and zinc metal (obs. = 36.3%, calc = 35.7%).

Ligand II was thermally decomposed in mainly decomposition steps within the temperature range successive

Table 4. The thermal data of 1,1-oxalylbis(4-phenylthiosemicarbazide) and its metal complexes.

Compound	Steps	Temperature range (˚C)	TG weight loss (%)		Assignment	T_{max}
			Calc. %	Found %		
(I)	1	25 - 237	42.40	42.50	2(N_2H_2), 2(HCNS) and $1/2O_2$ fragments	205 280 565
	2	237 - 337	30.40	30.20	$1/2O_2$and C_4H_4	
	3	More than 337	27.10	27.30	$C_{10}H_4$	
(Ia)	1	25 - 175	6.60	6.00	3 water	166 278 777 869
	2	175 - 390	28.50	29.20	2 acetone, 4 water and N_3H_3	
	3	390 - 707	18.90	18.30	($C_4N_3S_2$)	
	4	707 - 990	22.80	22.80	(C_9H_8)	
	5	More than 990	22.90	23.70	2CoO and residual carbon $3/2C_2$	
(Ib)	1,2	25 - 342	33.90	34.40	12water and 2(HCN)	187, 271 405, 480 840 978
	3	342 - 475	12.60	12.80	(CN_4S)	
	4,5	More than 475	53.40	52.80	($C_{13}H_{10}$), (S), (O_2) molecules and 2Cu(II) metal	
(Ic)	1	25 - 245	20.64	20.64	two water and two acetone molecules	228 319 493 649
	2	245 - 386	23.60	23.40	2(HCN), $2N_2$ and S_2	
	3	386 - 700	19.96	19.70	C_6H_4	
	4	More than 700	35.70	36.30	(C_8H_4), (ZnO) and zinc metal residue	
(Id)	1	25 - 226	12.40	12.60	two water and 2(HCN) molecules	224 301 530
	2	226 - 322	16.50	16.20	S_2 and $2N_2$	
	3	322 - 560	16.90	17.20	C_4H_4	
	4	More than 560	54.10	54.00	$C_{10}H_4$, (SnO) and Sn metal residue	

Table 5. The thermal data of 1,1-malonayl-bis(4-phenyl thiosemicarbazide) and its metal complexes.

Compound	Steps	Temperature ring (˚C)	TG weight loss (%)		Assignments	T_{max}/˚C
			Calc.	Found		
(II)	1	25 - 245	39.00	39.10	2(HNCO), $2H_2S$ and 2(NH) fragments	212
	2	245 - 345	32.50	32.80	2(HCN), (C_2H_2)	278
	3	More than 345	26.80	27.50	($C_{17}H_2$) residual	524
(IIa)	1	25 - 188	4.94	5.20	2 water	
	2	188 - 448	33.50	33.10	6 water molecules, $2N_2$, 2(HCN), and C_2H_2 fragments	242
	3	448 - 760	22.90	23.40	S_2 and O_2 molecules	477
	4	760 - 885	22.50	21.80	CH_4 and $C_{12}H_4$ fragments	854
	5	More than 885	16.50	17.30	Co_2 molecule is cobalt residue	959
(IIb)	1,2	25 - 245	15.40	16.40	6 water	181
	3	245 - 475	20.50	20.60	N_2, 2(HCN), N_2H_2, and O_2	277
	4	475 - 765	42.50	42.40	$C_{13}H_8$, S_2) fragments	506
	5	More than 765	21.50	20.60	Cu_2 metal residual	680
						974
(IIc)	1	25 - 224	15.300	15.50	6 water molecules	
	2	224 - 338	26.90	26.50	$2N_2$, S_2, $1/2O_2$ and 2(HCN) fragment	219
	3	338 - 643	18.20	18.60	$1/2O_2$, CH_4 and C_2H_2 molecules	309
	4	More than 643	39.50	39.40	residue metal of Zn_2 and $C_{12}H_4$ fragment	
(IId)	1,2	25 - 322	25.20	24.70	8 H_2O, HNCO and HCN molecules	
	3	322 - 506	8.80	9.30	$1/2S_2$ and HNCO	229
	4	506 - 589	9.10	9.56	NH_3, N_2 and $1/2S_2$ molecules	301
	5	More than 589	56.80	56.44	$C_{14}H_6$ and Sn_2 the residual metal	518

Table 6. The thermal data of 1,1-succinyl-bis(4-phenylthiosemi carbazide) and its metal complexes.

Compound	steps	Temperature range (˚C)	TG weight loss (%)		Assignment	T_{max}˚C
			Calc.	Found		
(III)	1	25 - 234	35.80	36.00	2(HCN), $2N_2$ and S_2 fragments	211
	2	234 - 334	32.30	32.10	O_2 and C_4H_6	276
	3	More than 334	31.70	31.90	$C_{12}H_{10}$	503
(IIIa)	1	25 - 332	32.00	31.90	6 water and 2(HCN) and N_2H_2	
	2	332 - 550	16.80	16.90	S_2, O_2 and C_2H_2	246
	3	550 - 895	24.80	24.60	C_8H_6	473
	4	More than 895	26.80	26.60	$3/2C_2$ and Co_2 metal	704
						828
(IIIb)	1	25 - 465	17.80	17.80	10water	
	2	465 - 700	14.80	15.00	2(HCN), $2N_2$ and $2(CH_2)$	208
	3	700 - 910	34.70	33.90	$2(C_6H_4)$ and $2S_2$	540
	4, 5	910 - 1000	32.60	33.27	Carbon and 4(CuO)	840
						977
(IIIc)	1	25 - 237	19.90	20.00	two water and two acetone molecules	
	2	237 - 365	25.38	25.30	2(HCN) 2(HNCO) 2CH and N_2 fragment	221
	3	More than 365	54.66	54.70	S_2, (C_6H_4) and Zn_2	348
						560
(IIId)	1	25 - 239	13.10	13.00	6 water molecules	
	2	239 - 321	13.30	12.70	2HCN and $2N_2$	226
	3,4	321 - 700	20.20	20.80	S_2 and O_2 fragments	302
	5	More than 700	53.40	53.50	residue metal of Sn_2 and contaminated of ($C_{16}H_{12}$) fragments	530
						572

decomposition steps at 25˚C - 700˚C. The first decomposition step (obs. = 39.14%, calc. = 39%) at 25˚C - 245˚C, may be attributed to the liberation of 2(HNCO), $2H_2S$ and 2(NH) fragments. The second decomposition step at 245˚C - 345˚C (obs. = 32.8%, calc. = 32.5%), is accounted for the removal of 2(HCN) and (C_2H_2). The decomposition of the ligand molecule ended with a final ($C_{17}H_2$) residue (obs. = 28%, calc = 28.3%).

The complex **IIa** was thermally decomposed in five steps within the temperature range 25˚C - 1000˚C. The first step (obs. = 5.2%, calc. = 4.94%) at 25˚C - 188˚C, may be attributed to the liberation of the two H_2O molecules. The second step at 188˚C - 448˚C (obs. = 33.1%, calc. = 33.5%), is accounted for the removal of $6H_2O$, $2N_2$, 2(HCN), and C_2H_2 fragments. The decomposition third step at 448˚C - 760˚C (obs. = 23.4%, calc = 22.9%) is accounted for the removal of $S_2$and O_2 molecules. The fourth step found at 760˚C - 885˚C (obs. = 21.8%, calc = 22.5%) is accounted for the removal of CH_4 and $C_{12}H_4$ fragments.

The TG curve of **IIb** complex indicates that the mass change begins at 25˚C and continuous up to 1000˚C. The first and second mass loss corresponds to the liberation of the 6 H_2O molecules (obs. = 16.4%, calc = 15.4%) at 25˚C - 245˚C. The third step occurs in the range 245˚C - 475˚C and corresponds to the loss of N_2, 2(HCN), N_2H_2, and O_2 (obs. = 20.6%, calc = 20.5%). The fourth step at 475˚C - 765˚C (obs. = 42.4%, calc = 42.5%) is accounted for the removal of ($C_{13}H_8$, S_2) fragments. The fifth steps are final decomposition organic ligand to the C_2 and Cu_2 residual (obs. = 20.6%, calc = 21.5%).

The complex **IIc** was thermally decomposed in mainly four steps within the temperature range 25˚C - 700˚C. The first decomposition step (obs. = 15.5%, calc = 15.3%) at 25˚C - 224˚C, may be attributed to the liberation of 6 H_2O. The second step at 224˚C - 338˚C (obs. = 26.5%, calc = 26.9%) is accounted for the removal of $2N_2$, S_2, $1/2O_2$ and 2(HCN) fragment. The decomposition third step found within the temperature 338˚C - 643˚C (obs. = 18.6%, calc = 18.2%) is accounted for the removal of $1/2O_2$, CH_4 and C_2H_2 fragments. The rest of the ligand molecule was removed and fourth the decomposition of the ligand molecule ended with a final residue metal of Zn_2 and $C_{12}H_4$ fragment (obs. = 39.4%, calc = 39.5%).

Ligand III was thermally decomposed in mainly decomposition steps within the temperature range successive decomposition steps within the temperature range 25˚C - 700˚C (**Figure 5**). The first decomposition step (obs. = 36%, calc. = 35.8%) within the temperature range 25˚C - 234˚C, may be attributed to the liberation of the 2(HCN), $2N_2$ and S_2 fragments. The second decomposition steps found within the temperature range 234˚C - 334˚C (obs. = 32.1%, calc. = 32.3%), which is reasonably accounted by the removal of O_2 and C_4H_6. The decomposition of the ligand molecule ended with a final $C_{12}H_{10}$ residue (obs. = 31.86%, calc = 31.7%).

The complex IIIa was thermally decomposed in four successive decomposition steps within the temperature range 25˚C - 1000˚C. The first decomposition step (obs. = 31.9%, calc. = 32%) within the temperature range 25˚C - 332˚C, may be attributed to the liberation of the 6water molecules, 2(HCN) and N_2H_2 fragments. The second decomposition steps found within the temperature range 332˚C - 550˚C (obs. = 16.9%, calc. = 16.8%), which is reasonably accounted by the removal S_2, O_2 and C_2H_2 fragments. The rest of the ligand molecule was removed and fourth the decomposition of the Co(II)/L complex molecule ended with a final $3/2C_2$ and Co_2 metal is cobalt residue (obs. = 26.6%, calc = 26.8%).

The TG curve of complex **IIIb** indicates that the mass change begins at 25˚C and continuous up to 1000˚C. The first mass loss corresponds to the liberation of the 12 water molecules (obs. = 17.8%, calc = 17.8%) within the temperature range 25˚C - 465˚C, (**Figure 6**). The second decomposition steps found within the temperature range 465˚C - 700˚C (obs. = 15%, calc. = 14.8%), which is reasonably accounted by the removal of 2(HCN), $2N_2$ and $2(CH_2)$ fragments. The decomposition fourth and fifth decomposition step are final decomposition organic ligand to the found within the temperature 910˚C-more than 1000˚C (obs. = 33.3%, calc = 32.6%) which is reasonably accounted for by the removal of carbon and 4(CuO), all the thermal diagrams in **Figure S12**.

6. Kinetic Studies

1,1-Oxalyl, 1,1-malonyl and 1,1-succinyl-bis-4-phenyl-thiosemicarbazide and all the metal Co(II), Cu(II), Zn(II) and Sn(II) complexes thermodynamic activation parameters of decomposition processes of the samples, namely activation energy, E^*, enthalpy, ΔH^*, entropy, ΔS^*, and Gibbs free energy change of the decomposition, ΔG^*, were evaluated graphically (**Figures S13-S27**) by employing the Coats-Redfern and Horowitz-Metzger relations [34]-[36]. All the thermodynamic parameters for the rest of materials, malonyl and Succinyl complexes were also calculated,. All the data for Kinetic thermal studies were summarized in **Tables 7-9**. The high values of the activation energy illustrated to the thermal stability of the complexes. The activation energies of decomposition

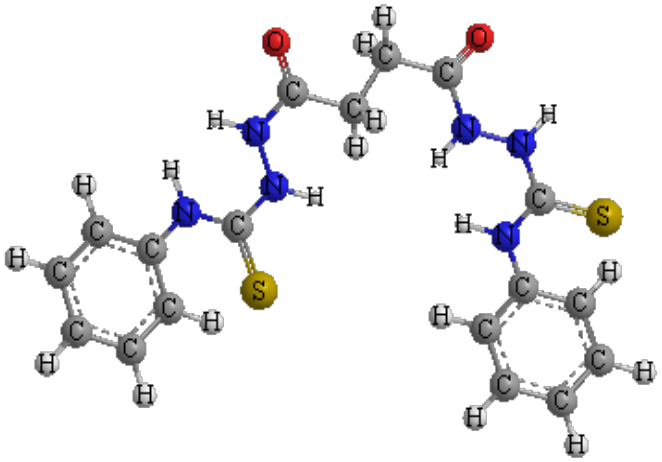

Figure 5. 1,1-Succinyl-bis(4-phenylthiosemicarbazide) (III). Ph-NH-CS-NH-NH-CO-CH_2-CH_2-CO-NH-NH-CS-NH-Ph.

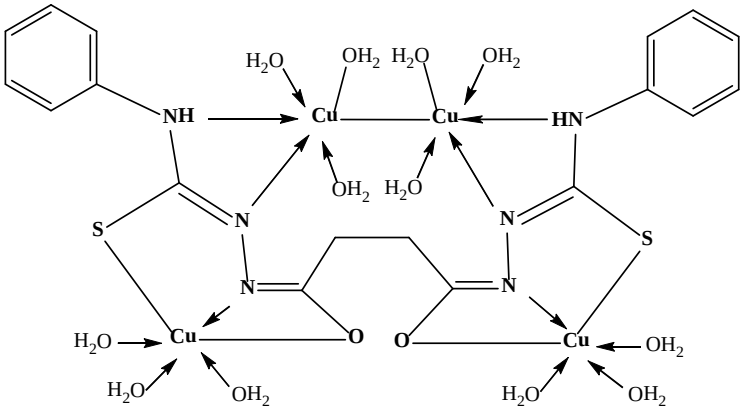

Figure 6. 1,1-Succinyl bis-4-phenylthiosemicarbazide) Tris-copper trihydrate (**IIIb**).

were in the range 55 - 450 kJ·mol^{-1}. The high values of the activation energy illustrated to the thermal stability of the complexes. ΔG is positive for reaction for which ΔH is positive and ΔS is negative. The reaction for which ΔG is positive and ΔS is negative considered as unfavorable or non spontaneous reactions. Reactions are classified as either exothermic (ΔH < 0) or endothermic (ΔH > 0) on the basis of whether they give off or absorb heat. Reactions can also be classified as exergonic (ΔG < 0) or endergonic (ΔG > 0) on the basis of whether the free energy of the system decreases or increases during the reaction. The thermodynamic data obtained with the two methods are in harmony with each other. The activation energy of all 1,1-oxalyl-bis (4-phenyl) thiosemicarbazide and its Co^{2+}, Cu^{2+}, Zn^{2+} and Sn^{2+} complexes is expected to increase in relation with decrease in their radii (Tunali and Ozkar 1993). The smaller size of the ions permits a closer approach of the ligand (H_4OxTSC). Hence, the E value in the first stage for the Zn^{2+} complex is higher than that for the other Sn^{2+}, Cu^{2+} and Co^{2+} complex. The correlation coefficients of the Arrhenius plots of the thermal decomposition steps were found to lie in the range 0.9925 to 0.9995 showing a good fit with linear function. It is clear that the thermal decomposition process of all complexes is non-spontaneous, *i.e.*, the thermal stability of the complexes. The activation energy of Ligand **II** and its Co^{2+}, Cu^{2+}, Zn^{2+} and Sn^{2+} complexes is expected to increase in relation with decrease in their radii. The high values of the activation energy illustrated to the thermal stability of the complexes. The data were calculated and are summarized in **Table 8**. The smaller size of the ions permits a closer approach of the ligand (H_4MaTSC). Hence, the E value in the first stage for the Zn^{2+} complex is higher than that for the other Sn^{2+}, Cu^{2+} and Co^{2+} complex. The activation energies of **III** and its metal complexes are summarized in **Table 9**. The high values of the activation energy illustrated to the thermal stability of the complexes. It is clear that the

Table 7. Kinetic parameters using the Coats-Redfern (CR) and Horowitz-Metzger (HM) operated for (H_4OxTS) and its complexes.

Complex	Stage	Method	Parameter					r
			E (J mol^{-1})	A (s^{-1})	ΔS (J·mol^{-1}·K^{-1})	ΔH (J·mol^{-1})	ΔG (J·mol^{-1})	
(I)	1st	CR	1.12×10^5	1.07×10^{10}	-5.68×10^1	1.08×10^5	1.35×10^5	0.9981
		HM	1.28×10^5	1.50×10^{12}	-1.58×10^1	1.24×10^5	1.32×10^5	0.9961
(Ia)	1st	CR	5.14×10^4	7.99×10^3	-1.75×10^2	4.68×10^4	1.43×10^5	0.9920
		HM	6.33×10^4	6.60×10^3	-1.77×10^2	5.87×10^4	1.56×10^5	0.9929
(Ib)	1st	CR	1.10×10^5	7.01×10^9	-6.04×10^1	1.06×10^5	1.35×10^5	0.9995
		HM	1.31×10^5	2.96×10^{12}	-1.01×10^1	1.27×10^5	1.31×10^5	0.9991
(Ic)	1st	CR	8.04×10^4	7.21×10^5	-1.38×10^2	7.59×10^4	1.50×10^5	0.9968
		HM	1.07×10^5	2.29×10^8	-8.98×10^1	1.02×10^5	1.51×10^5	0.9985
(Id)	1st	CR	8.61×10^4	1.65×10^7	-1.11×10^2	8.2×10^4	1.37×10^5	0.9938
		HM	1.71×10^5	32.75×10^9	-6.59×10^1	1.05×10^5	1.38×10^5	0.9955

Table 8. Kinetic parameters using the Coats-Redfern (CR) and Horowitz-Metzger (HM) operated for: (H_4MaTS) and its Co(II), Cu(II), Zn(II) and Sn(II) complexes.

Complex	Stage	Method	Parameter					r
			E (J·mol^{-1})	A (s^{-1})	ΔS (J·mol^{-1}·K^{-1})	ΔH (J·mol^{-1})	ΔG (J·mol^{-1})	
(II)	1st	CR	1.79×10^5	1.94×10^{17}	8.20×10^1	1.75×10^5	1.35×10^5	0.9997
		HM	1.54×10^5	7.15×10^{14}	3.54×10^1	1.50×10^5	1.33×10^5	0.9992
(IIa)	1st	CR	4.70×10^4	1.40×10^2	-2.08×10^2	4.27×10^4	1.50×10^5	0.9963
		HM	6.65×10^4	4.13×10^4	-1.61×10^2	6.22×10^4	1.45×10^5	0.9956
(IIb)	1st	CR	6.07×10^4	2.32×10^3	-1.86×10^2	5.61×10^4	1.58×10^5	0.9931
		HM	6.87×10^4	2.35×10^4	-1.66×10^2	6.42×10^4	1.55×10^5	0.9918
(IIc)	1st	CR	4.58×10^4	1.17×10^{47}	6.52×10^2	4.54×10^5	1.33×10^5	0.9977
		HM	4.65×10^5	1.20×10^{48}	6.70×10^2	4.61×10^5	1.30×10^5	0.9982
(IId)	1st	CR	2.76×10^4	1.68×10^{27}	2.72×10^2	2.72×10^5	1.36×10^5	0.9950
		HM	2.95×10^5	1.77×10^{29}	3.11×10^2	2.90×10^5	1.35×10^5	0.9945

Table 9. Kinetic parameters using the Coats-Redfern (CR) and Horowitz-Metzger (HM) operated for 1,1-succinyl-bis (phenylthiosemicarbazide) and its Co(II), Cu(II), Zn(II) and Sn(II) complexes.

Complex	Stage	Method	Parameter					r
			E (J·mol^{-1})	A (s^{-1})	ΔS (J·mol^{-1}·K^{-1})	ΔH (J·mol^{-1})	ΔG (J·mol^{-1})	
(III)	1st	CR	3.23×10^5	1.82×10^{33}	3.88×10^2	3.19×10^5	1.31×10^5	0.9984
		HM	3.51×10^5	2.96×10^{36}	4.49×10^2	3.47×10^5	1.29×10^5	0.9989
(IIIa)	1st	CR	4.56×10^4	1.31×10^2	-2.09×10^2	4.13×10^4	1.50×10^5	0.9988
		HM	5.49×10^4	2.02×10^3	-1.86×10^2	5.05×10^4	1.47×10^5	0.9953
(IIIb)	3st	CR	1.67×10^5	5.30×10^5	-1.46×10^2	1.57×10^5	3.20×10^5	0.9993
		HM	2.13×10^5	5.28×10^7	-1.08×10^2	2.04×10^5	3.24×10^5	0.9985
(IIIc)	1st	CR	1.95×10^5	5.85×10^{18}	1.10×10^2	1.91×10^5	1.37×10^5	0.9992
		HM	2.06×10^5	1.77×10^{20}	1.39×10^2	2.02×10^5	1.34×10^5	0.9974
(IIId)	1st	CR	8.08×10^4	3.72×10^6	-1.23×10^2	7.66×10^4	1.38×10^5	0.9984
		HM	9.84×10^4	2.60×10^8	-8.81×10^1	9.43×10^4	1.38×10^5	0.9984

thermal decomposition process of compounds **I**, **II**, **III** and Co^{2+}, Cu^{2+}, Zn^{2+}, Sn^{2+} metal complexes are non-spontaneous, *i.e.*, the materials are thermally stable.

7. Antimicrobial Activity

Three compounds were tested in vitro for their antibacterial activities against four strains of bacteria Gram nega-

tive *Escherichia coli*, *Pseudomonas aeruginosa* species and gram-positive *Bacillus cereus* and *Staphylococcus aureus*. The bacteria were maintained on nutrient agar media. The minimal inhibitory concentration of some of the tested compounds was measured by a threefold serial dilution method. The screening results indicate that not all the compounds exhibited antibacterial activities. In this study, the tested compounds oxalyl, malonyl, and succinyl bis-4-phenylthiosemicarbazide were active against both *Bacillus cereus*, *Staphylococcus aureus* which are Gram-positive bacteria as well as *Escherichia coli and Pseudomons aeruginose* which are Gram-negative bacteria. However, the antibacterial activity was very pronounced against the Gram-negative bacteria and could be classified in the order of very good activity.

8. Conclusion

The activation energies of decomposition of 1,1-oxalyl, 1,1-malonyl and 1,1-succinyl-bis-4-phenyl-thiosemicarbazide and all the metal complexes are calculated. The data are summarized in **Tables 7-9**. The high values of the activation energy are illustrated to the thermal stability of the complexes. It is clear that the thermal decomposition process of all 1,1-oxalyl-bis-4-phenylthiosemicarbazide (H_4OxTSC) and its complexes is thermally stable. The activation energy of Ligand **II** and its Co^{2+}, Cu^{2+}, Zn^{2+} and Sn^{2+} complexes are expected to increase in relation with decrease in their radii. The high values of the activation energy are illustrated to the thermal stability of the complexes. The data are calculated and are summarized in **Table 7**, **Table 8**. The smaller size of the ions permits a closer approach of the ligand (H_4MaTSC). Hence, the E value in the first stage for the Zn^{2+} complex is higher than that for the other Sn^{2+}, Cu^{2+} and Co^{2+} complex. The activation energies of III and its metal complexes are summarized in **Table 9**. The high values of the activation energy are illustrated to the thermal stability of the complexes. It is clear that the thermal decomposition process of compounds **I**, **II**, **III** and Co^{2+}, Cu^{2+}, Zn^{2+}, Sn^{2+} metal complexes are non-spontaneous, *i.e.*, the materials are thermally stable. The tested compound **I**, **II** and **III** show a good activity against four strains of bacteria Gram negative *Escherichia coli*, *Pseudomonas aeruginosa* species and Gram-positive *Bacillus cereus* and *Staphylococcus aureus.*

References

[1] Preston, J.B. (1955) Pentylenetetrazole AND Thiosemicarbazide: A Study of Convulsant Activity in the Isolated Cerebral Cortex Preparation, *Journal of Pharmacology.*

[2] DeConti, R.C., Toftness, B.R., Agrawal, K.C., *et al*. (1972) Clinical and Pharmacological Studies with 5-Hydroxy-2-formylpyridine Thiosemicarbazone. *Cancer Research*, **32**, 1455-1462.

[3] Lobana, T.S., Butcher, R.J., Castineiras, A., Bermejo, E. and Bharatam, Prasad V. (2006) Bonding Trends of Thiosemicarbazones in Mononuclear and Dinuclear Copper(I) Complexes: Syntheses, Structures, and Theoretical Aspects. *Inorganic Chemistry*, **45**, 1535-1542.

[4] Zhao, Y. (2000) Liquid Chromatographic Determination of Chelates of Cobalt(II), Copper(II) and Iron(II) with 2-Thiophenecarboxaldehyde-4-phenyl-3-thiosemicarbazone. *Chromatographia*, **51**, 231-234. http://dx.doi.org/10.1007/BF02490570

[5] Khuhawar, M.Y. and Lanjwani, S.N. (1998) Liquid Chromatographic Determination of Cobalt(II), Copper(II) and Iron(II) Using 2-Thiophenaldehyde-4-phenyl-3-thiosemicarbazone as Derivatizing Reagent. *Talanta*, **46**, 485-490. http://dx.doi.org/10.1016/S0039-9140(97)00213-0

[6] Lunn, G., Phillips, L.R. and Pacula-Cox, C. (1998) Reversed-Phase High-Performance Liquid Chromatography of 4-(2-Pyridyl)-1-piperazinethiocarboxylic Acid 2-[1-(Pyridyl)ethylidene]hydrazide dihydrochloride (NSC 348977), a Synthetic Thiosemicarbazone with Antitumor Activity. *Journal of Chromatography B*: *Biomedical Sciences and Applications*, **708**, 217-222. http://dx.doi.org/10.1016/S0378-4347(97)00637-3

[7] Hoshi, S., Higashihara, K., Suzuki, M., Sakurada, Y., Sugawara, K., Uto, M. and Akatsuka, K. (1997) Simultaneous Determination of Platinum(II) and Palladium(II) by Reversed Phase High-Performance Liquid Chromatography with Spectrophotometric Detection after Collection on and Elution from Resin Coated with Dimethylglyoxal Bis (4-phenyl-3-thisomicarbazone). *Talanta*, **44**, 571-576. http://dx.doi.org/10.1016/S0039-9140(96)02064-4

[8] Gismera, M.J., Mendiola, M.A., Procopio, J.R. and Sevilla, M.T. (1999) Copper Potentiometric Sensors Based on Copper Complexes Containing Thiohydrazone and Thiosemicarbazone Ligands. *Analytica Chimica Acta*, **385**, 143-149. http://dx.doi.org/10.1016/S0003-2670(98)00840-X

[9] Qu, J.Y., Liu, M. and Liu, K.Z. (1999) Simultaneous Determination of Lead and Copper by Carbon Paste Electrodes Modified with Pyruvaldehyde Bis(NN'-Dibutyl Thiosemicarbazone). *Analytical Letters*, **32**, 1991-2006. http://dx.doi.org/10.1080/00032719908542947

[10] Tang, B., Du, M., Sun, Y., Xu, H.L. and Shen, H.X. (1998) The Study and Application of Biomimic Peroxidase Ferric 2-Hydroxy-1-naphthaldehyde Thiosemicarbazone. *Talanta*, **47**, 361-366. http://dx.doi.org/10.1016/S0039-9140(98)00149-0

[11] West, D.X., Carlson, C.S., Liberta, A.E. and Scovil, J.P. (1990) The Chemical and Antifungal Properties of the Copper (II) Complexes of 2-Acetyl-pyrazine ^{4}N-methyl-, ^{4}N-dimethyl-, and 3-Hexamethyleneiminyl-thiosemicarbazone. *Trans. Metchem*, **15**, 383-387. http://dx.doi.org/10.1007/BF01177467

[12] West, D.X., Carlson, C.S., Liberta, A.E., Albert, J.N. and Daniel, C.R. (1990) Transtion Metal Ion Complexes of Thiosemicarbazones Derived from 2-Acetylpyridine. *Transition Metal Chemistry*, **15**, 341-344. http://dx.doi.org/10.1007/BF01177458

[13] Mandour, A.H., Fawzy, N.M., El-Shihi, T.H. and El-Bazza, Z.E. (1995) Synthesis, Antimicrobial and Antiaflatoxigenic Activities of Some Benzofuran Containing 1,2,4-Triazole, 1,3,4-Thiadiazole and Oxadiazole Derivatives. *Pakistan Journal of Scientific and Industrial Research*, **38**, 402-406.

[14] Liu, M.C., Lin, T.S., Penketh, P. and Sartorelli, A.C. (1995) Synthesis and Antitumor Activity of 4- and 5-Substituted Derivatives of Isoquinoline-1-carboxaldehyde Thiosmicarbazone. *Journal of Medicinal Chemistry*, **38**, 4234-4243. http://dx.doi.org/10.1021/jm00021a012

[15] Liu, M.C., Lin, T.S., Cory, J.G., Cory, A.H. and Sartorelli, A.C. (1996) Synthesis and Biological Activity of 3- and 5-Amino Derivatives of Pyridine-2-carboxaldehyde Thiosemicarbazone. *Journal of Medicinal Chemistry*, **39**, 2586-2593. http://dx.doi.org/10.1021/jm9600454

[16] Zhu, X., Wang, C., Lu, Z., Dang, Y. (1997) Synthesis Characterization and Biological Activity of the Schiffbase Derived from 3,4-Dihydroxybenz-aldehyde and Thiosemicarbazide, and Its Metal Complexes with Nickel(II) and Iron(II). *Transition Metal Chemistry* (*London*), **22**, 9-13. http://dx.doi.org/10.1023/A:1018453316348

[17] Lim, J.K., Mathias, C.J. and Green, A.M.J. (1997) Mixed Bis(thiosemicarbazone) Ligands for the Preparation of Copper Radiopharmaceuticals: Synthesis and Evaluation of Tetradentate Ligands Containing Two Dissimilar Thiosemicarbazone Functions. *Journal of Medicinal Chemistry*, **40**, 132-136. http://dx.doi.org/10.1021/jm9605703

[18] Amin, R.R., Yamany, Y.B., Abo-Aly, M.M. and Hassan, A.M.A. (2011) Kinetic Parameters for Thermal Decomposition for Novel 1,1-Malonyl bis(4-p-chlorophenylthiosemicarbazide and Cu(II), Co(II), Zn(II) and Sn(II) Complexes Synthesized by Electrochemical Method. *Natural Science*, **3**, 783-794. http://dx.doi.org/10.4236/ns.2011.39103

[19] El-Shekeil, A., Al-Yusufy, F., Amin, R.R. and Abdullah, A.-H. (2004) The DC Electrical Conductivity of the Direct Electrochemically Synthesized Poly (Azomethinethiosemicarbazone)-Metal Complexes. *Journal of Inorganic and Organometallic Polymers*, **14**, 131-148. http://dx.doi.org/10.1023/B:JOIP.0000028091.50660.3a

[20] El-Asmy, A.A., Al-Ansi, T.Y., Amin, R.R. and El-Shahat, M.F. (1990) Structural Studies on Cadmium(II), Cobalt(II), Copper(II) Nickel(II) and Zinc(II) Complexes of 1-Malonyl bis(4-phenylthiosemicarbazide). *Transition Metal Chemistry*, **15**, 12-15.

[21] El-Asmy, A.A., Al-Ansi, T.Y., Amin, R.R. and Mounir, M. (1990) Spectral, Magnetic and Electrical Properties of 1-Succinyl Bis(4-phenylthiosemicarbazide) Complexes. *Polyhedron*, **9**, 2029-2034. http://dx.doi.org/10.1016/S0277-5387(00)84032-2

[22] Mostafa, M.M. (2007) Spectroscopic Studies of Some Thiosemicarbazide Compounds Derived from Girard's T and P. *Spectrochimica Acta Part A*: *Molecular and Biomolecular Spectroscopy*, **66**, 480-486. http://dx.doi.org/10.1016/j.saa.2006.02.063

[23] Elreedy, A.A.M. and Amin, R.R. (2015) Chemical and Electrochemical Preparation for Some Metal(II) Complexes of Some Pyridine-2-(1H)-thione-3-cyano-4-(2-methylphenyl)-5,6-Ring. *Fused Cycloalkane Derivatives*, **6**.

[24] Amin, R.R. and El-Gemeie, G.E.H. (2001) The Direct Electrochemical Synthesis of Co(II), Ni(II) and Cu(II) Complexes of Some Pyridinethione Derivatives. *Synthesis and Reactivity in Inorganic and Metal-Organic Chemistry*, **31**, 431-440. http://dx.doi.org/10.1081/SIM-100002230

[25] El-Metwally, N.M., El-Shazly, R.M., Gabr, I.M. and El-Asmy, A.A. (2005) Physical and Spectroscopic Studies on Novel Vanadyl Complexes of Some Substituted Thiosemicarbazides. *Spectrochimica Acta Part A*: *Molecular and Biomolecular Spectroscopy*, **61**, 1113-1119. http://dx.doi.org/10.1016/j.saa.2004.06.027

[26] Novaković, S.B., Bogdanović, G.A. and Leovac, V.M. (2006) Transition Metal Complexes with Thiosemicarbazide-Based Ligands. Part L. Synthesis, Physicochemical Properties and Crystal Structures of Co(II) Complexes with Acetone *S*-Methyliso-Thiosemicarbazone. *Polyhedron*, **25**, 1096-1104.

[27] Novaković, S.B., Bogdanović, G.A. and Leovac, V.M. (2005) Transition Metal Complexes with Thiosemicarbazide-Based Ligands. XLIV. The Supramolecular Arrangement in the Ni(II) Complexes of *S*-Methylisothiosemicarbazide. *Inorganic Chemistry Communications*, **8**, 9-13.

[28] Leovac, V.M., Novaković, S.B., Bogdanović, G.A., Joksović, M.D. and Mészáros, K. (2007) Transition Metal Complexes

with Thiosemicarbazide-Based Ligands. Part LVI: Nickel(II) Complex with 1,3-Diphenylpyrazole-4-carboxaldehyde Thiosemicarbazone and Unusually Deformed Coordination Geometry. *Polyhedron*, **26**, 3783-3792. http://dx.doi.org/10.1016/j.poly.2007.04.012

[29] Refat, M., Al-Azab, F., Mudamma, H., Amin, R.R. and Jameel, Y. (2014) Preparation, Spectroscopic and Thermal Characterization of New La(III), Ce(III), Sm(III) and Y(III) Complexes of Enalapril Maleate Drug. *In Vitro* Antimicrobial Assessment Studies. *Journal of Molecular Structure*, **1059**, 208-224. http://dx.doi.org/10.1016/j.molstruc.2013.12.003

[30] El-Asmy, A.A., Al-Gammal, O.A., Dena, A.S. and Ghazy, S.E. (2009) Synthesis, Characterization, Molecular Modeling and Eukaryotic DNA Degradation of 1-(3,4-Dihydroxybenzylidene) Thiosemicarbazide Complexes. *Journal of Molecular Structure*, **934**, 9-22. http://dx.doi.org/10.1016/j.molstruc.2009.05.039

[31] Hassaneien, M.M., Gabr, I.M., Abdel-Rhman, M.H. and El-Asmy, A.A. (2008) Synthesis and Structural Investigation of Mono- and Polynuclear Copper Complexes of 4-Ethyl-1-(pyridin-2-yl) Thiosemicarbazide. *Spectrochimica Acta Part A*, **71**, 73-79. http://dx.doi.org/10.1016/j.saa.2007.11.009

[32] Chandra, S. and Kumar, U. (2005) Spectral and Magnetic Studies on Manganese(II), Cobalt(II) and Nickel(II) Complexes with Schiff Bases. *Spectrochimica Acta*, *Part A*, **61**, 219-224. http://dx.doi.org/10.1016/j.saa.2004.03.036

[33] Chohan, Z.H. (2009) Metal-Based Antibacterial and Antifungal Sulfonamides: Synthesis, Characterization, and Biological Properties. *Transition Metal Chemistry*, **34**, 153-161. http://dx.doi.org/10.1007/s11243-008-9171-y

[34] Refat, M.S., El-Deen, I.M., Amin, R.R. and El-Ghol, S. (2010) Spectroscopic Studies and Biological Evaluation of Some Transition Metal Complexes of a Novel Schiff Base Ligands Derived From 5-Arylazo-Salicyladehyde and *O*-Amino Phenol. *Toxicological & Environmental Chemistry*, **92**, 1093-1110. http://dx.doi.org/10.1080/02772240903252173

[35] Refat, M.S., Al-Maydama, H.M.A., Al-Azab, F., Amin, R.R. and Jamil, Y.M.S. (2014) Synthesis, Thermal and Spectroscopic Behaviors of Metal-Drug Complexes: La(III), Ce(III), Sm(III) and Y(III) Amoxicillin Trihydrate Antibiotic Drug Complexes. *Spectrochimica Acta Part A*: *Molecular and Biomolecular Spectroscopy*, **128**, 427-446.

[36] Refat, M., Amin, R.R., Jameel, Y., Al-Azab, F. and Mudam, H. (2014) Synthesis and *in Vitro* Microbial Evaluation of La(III), Ce(III), Sm(III) and Y(III) Metal Complexes of Vitamin B6 Drug. *Spectrochimica Acta Part A*: *Molecular and Biomolecular Spectroscopy*, **127**, 196-215. http://dx.doi.org/10.1016/j.saa.2014.02.043

Appendix

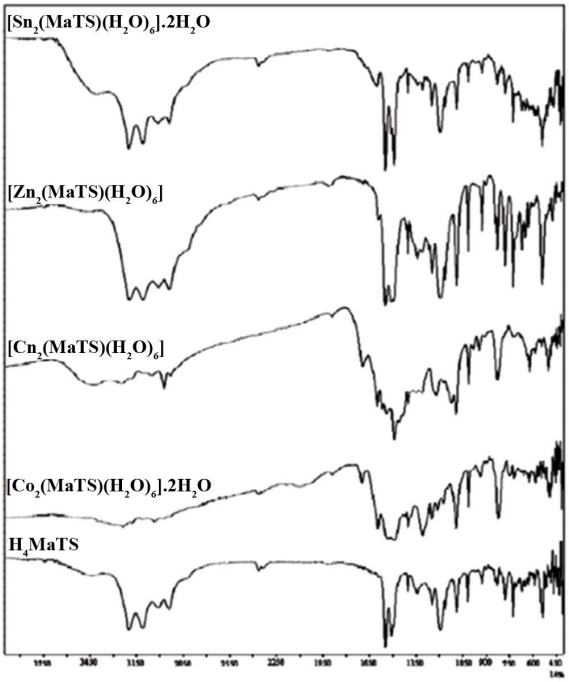

Figure S1. IR spectra for 1, 1-Malonyl bis-4phenyl thiosemicarbazide and its metal complexes.

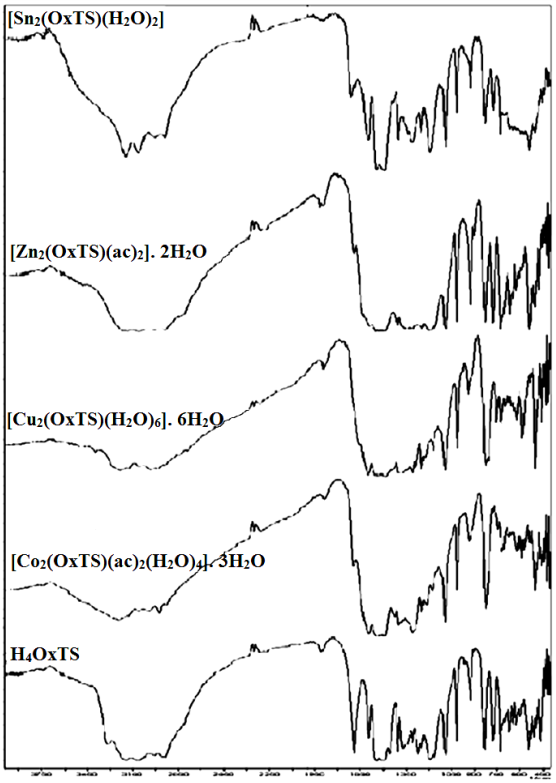

Figure S2. IR spectra for 1,1-Oxalyl bis-4phenyl thiosemicarbazide and its metal complexes.

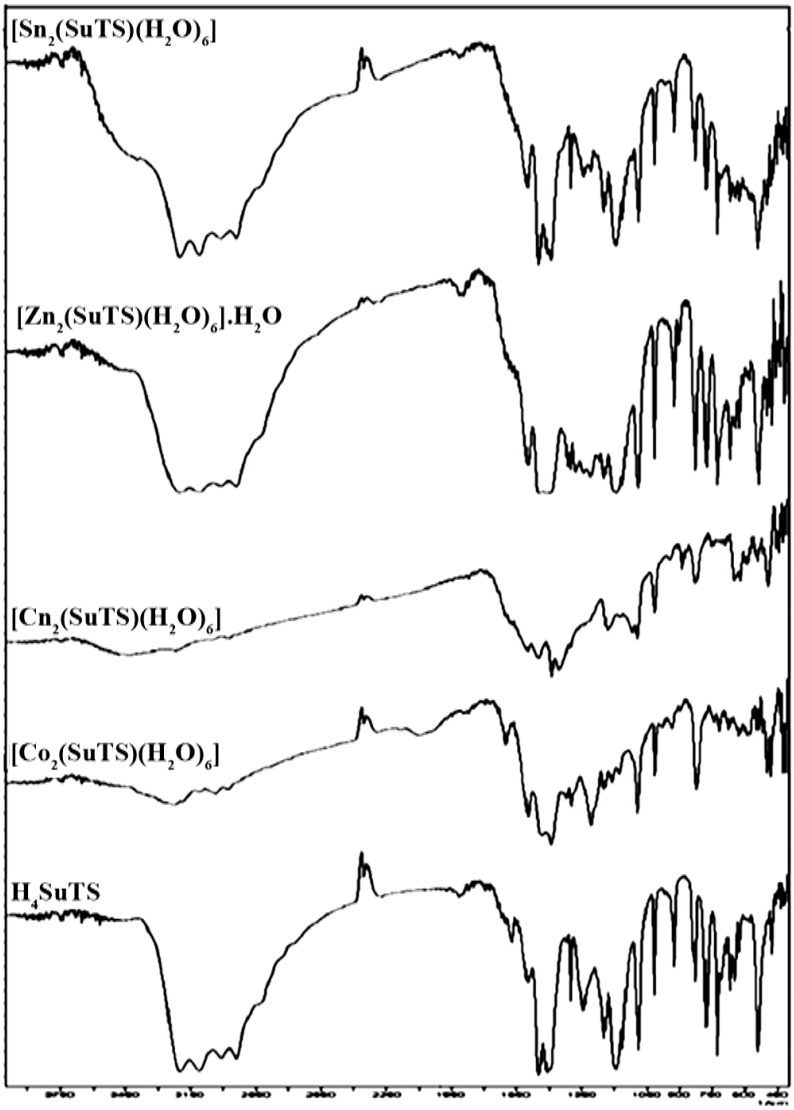

Figure S3. IR spectra for 1, 1-Succinyl bis-4phenyl thiosemicarbazide and its metal complexes.

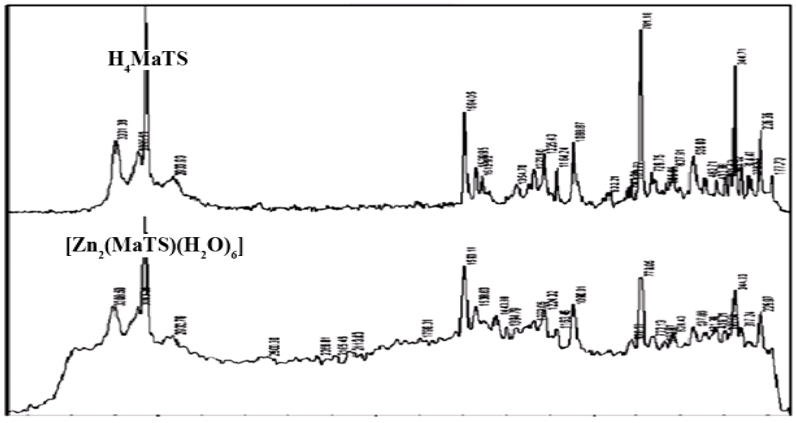

Figure S4. Raman spectra for 1, 1-Malonylbis-4phenyl thiosemicarbazide and Zinc-metal complex.

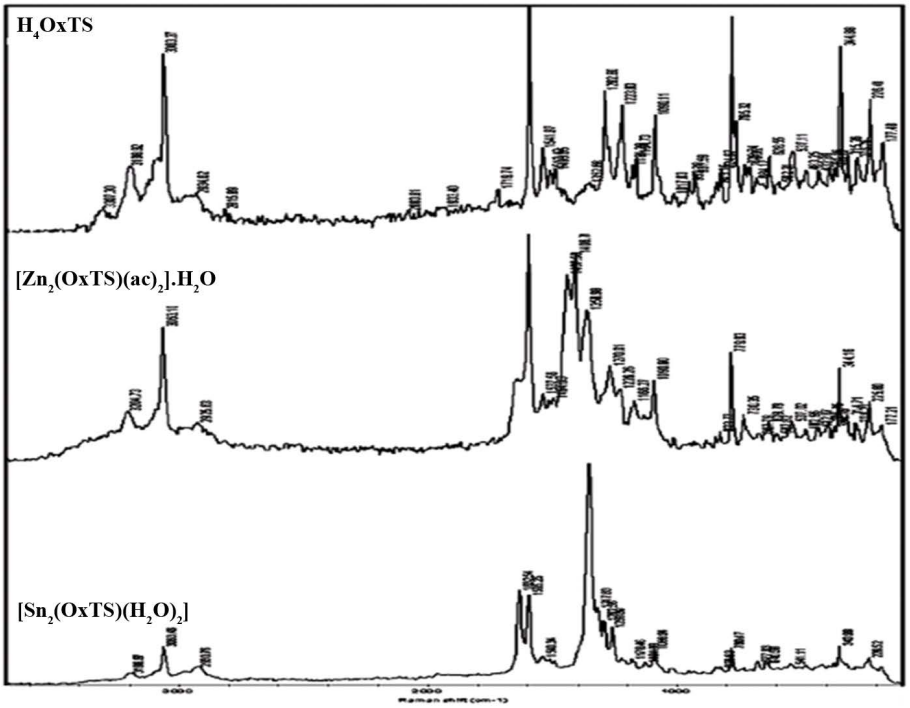

Figure S5. Raman spectra for 1, 1-Oxalaylbis-4phenylthiosemicarbazide, Zinc and Tin-metal complexes.

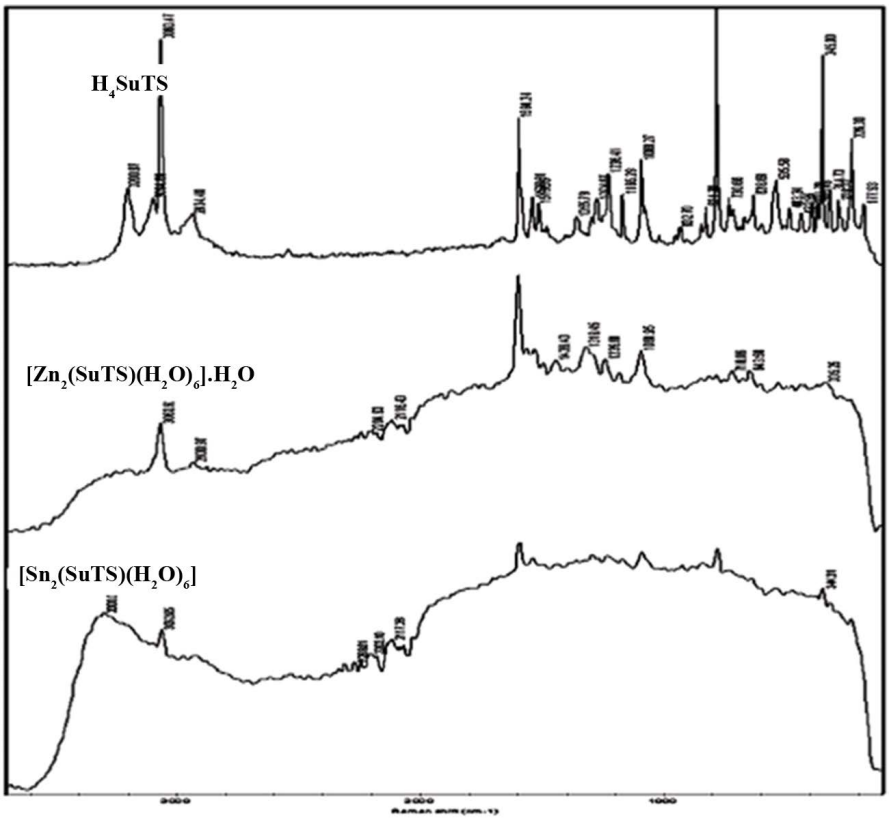

Figure S6. Raman spectra for 1, 1-Oxalaylbis-4phenylthiosemicarbazide, Zinc and Tin-metal complexes.

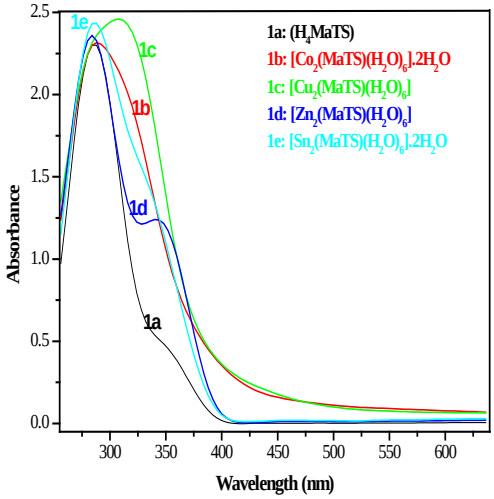

Figure S7. Ultraviolet and Visible spectra diagram of 1,1-Malonyl-bis (4-phenyl thiosemicarbazide) and its metal complexes.

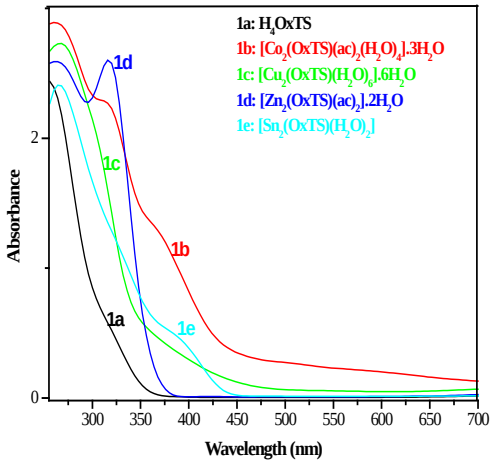

Figure S8. Ultraviolet and Visible spectra diagram of 1,1-Oxalyl-bis (4-phenyl thiosemicarbazide) and its metal complexes.

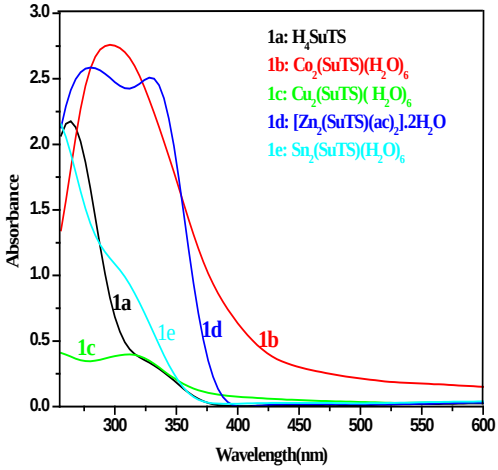

Figure S9. Ultraviolet and Visible spectra diagram of 1,1-Succinyl-bis(4-phenyl thiosemicarbazide) and its metal complexes.

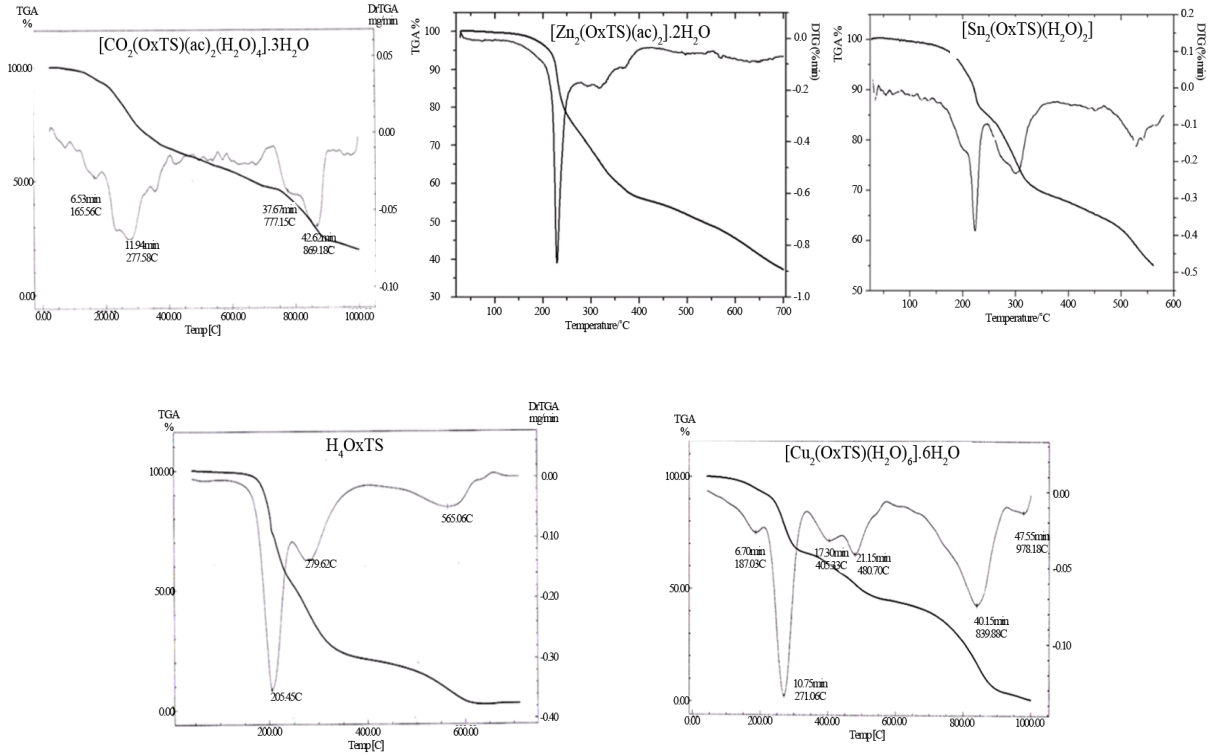

Figure S10. TGA and DTGA diagram of 1,1-oxalyl-bis(4- phenyl thiosemicarbazide), H_4OxTSC and its metal complexes.

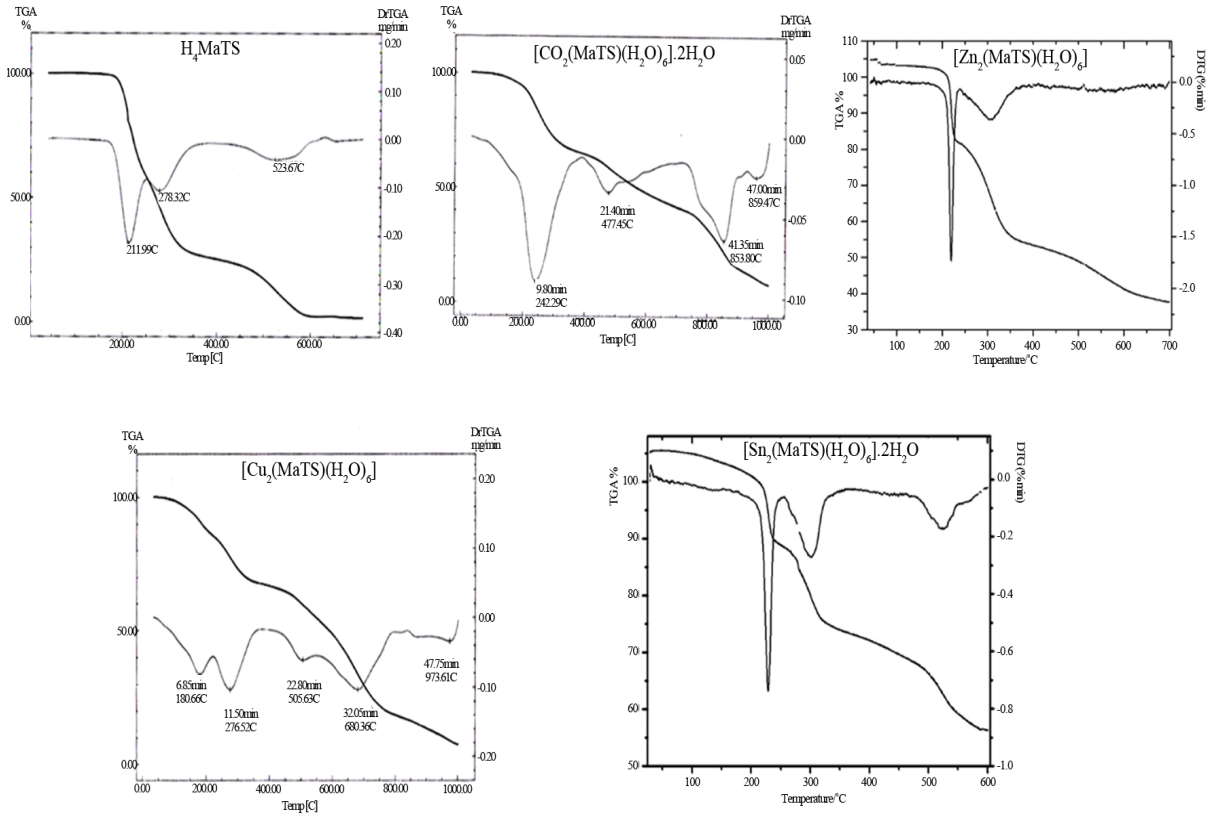

Figure S11. TGA and DTGA diagram of 1,1-malonayl-bis(4-phenyl thiosemicarbazide), H_4MaTSC and its metal complexes.

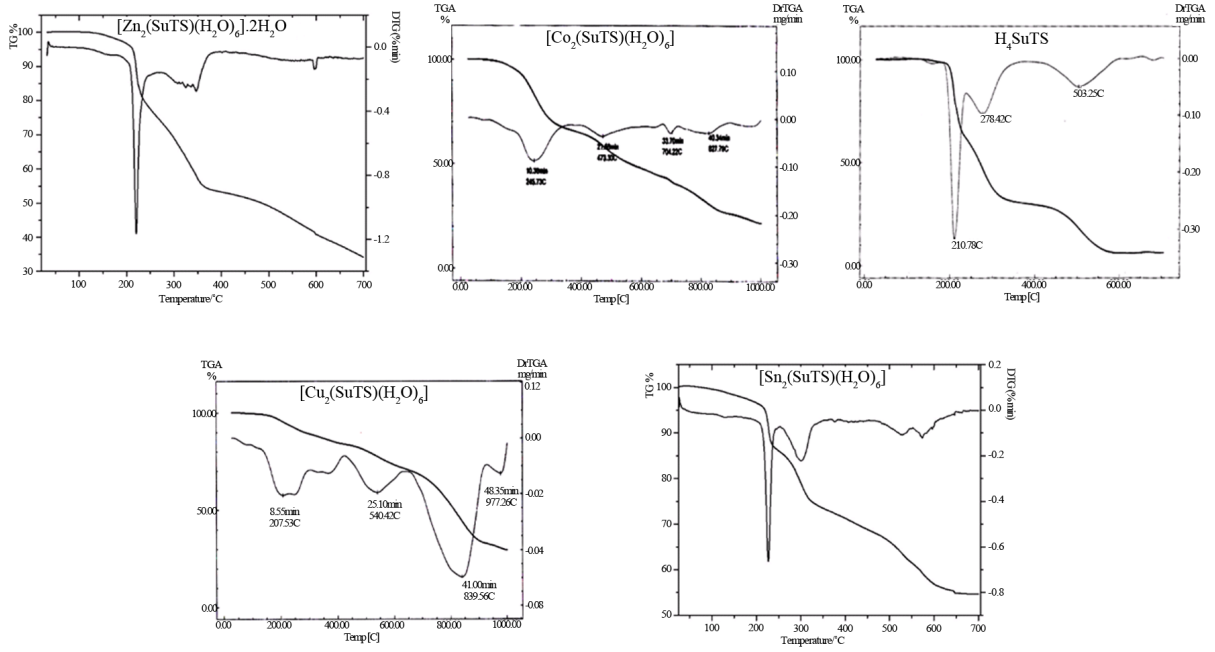

Figure S12. TGA and DTGA diagram of 1,1-succinyl-bis(4- phenyl thiosemicarbazide), H_4SuTSC and its metal complexes.

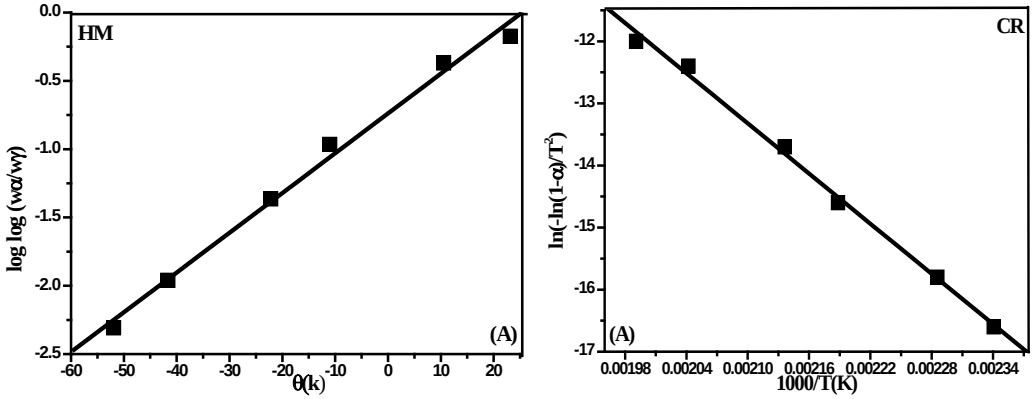

Figure S13. Kinetic data curves of: 1,1-Oxalyl-bis(4-phenyl thiosemicarbazide).

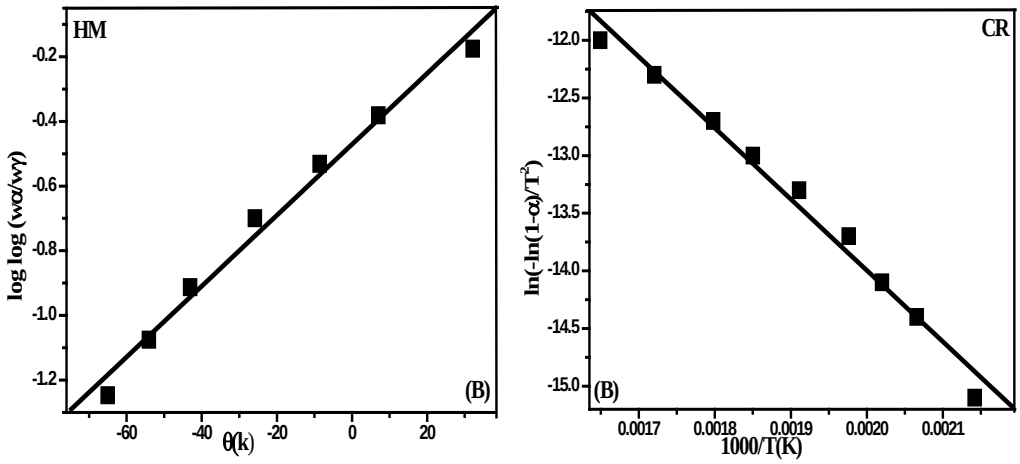

Figure S14. Kinetic data curves of: $[Co_2OxTS\ (ac)_2(H_2O)_4]\cdot 3H_2O$ complex.

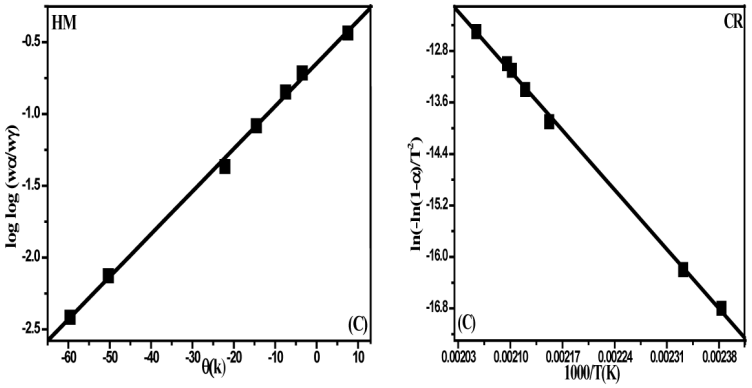

Figure S15. Kinetic data curves of $[Cu_2OxTS(H_2O)_6]\cdot 6H_2O$ complex.

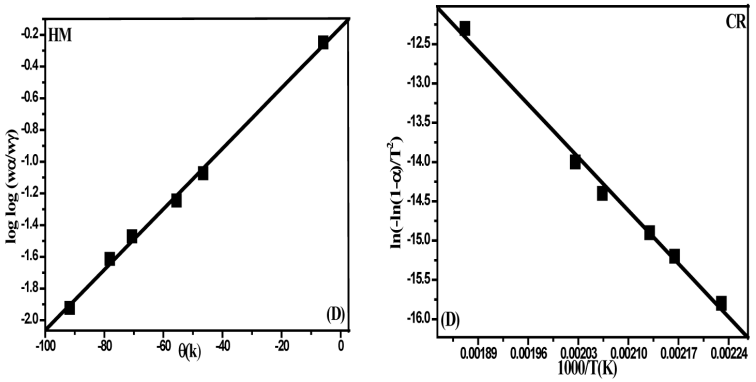

Figure S16. Kinetic data curves of: $[Zn_2OxTS(ac)_2]\cdot 2H_2O$ complex.

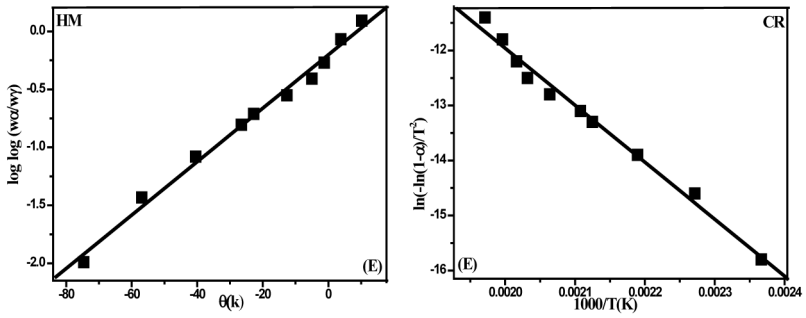

Figure S17. Kinetic data curves of $[Sn_2OxTS(H_2O)_2]$ complex.

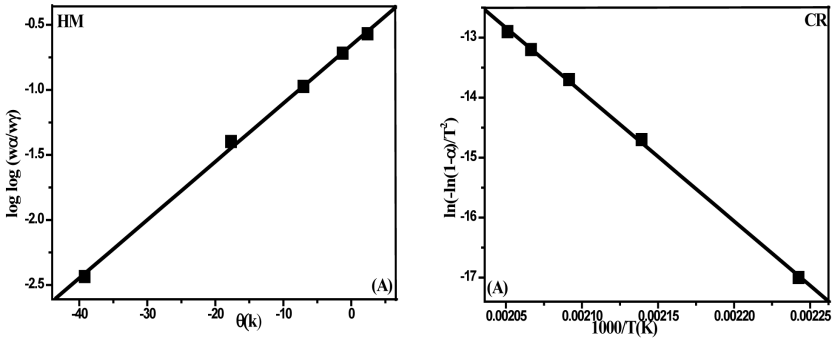

Figure S18. Kinetic data curves of 1,1-Malonayl-bis(4-phenyl thiosemicarbazide).

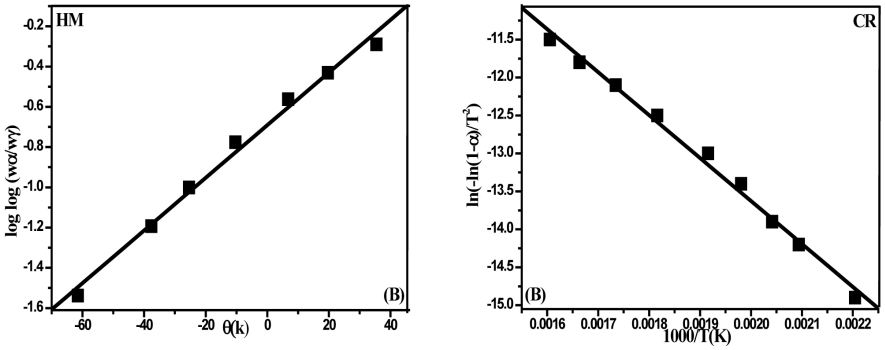

Figure S19. Kinetic data curves of $[Co_2MaTS(H_2O)_6]\cdot 2H_2O$ complex.

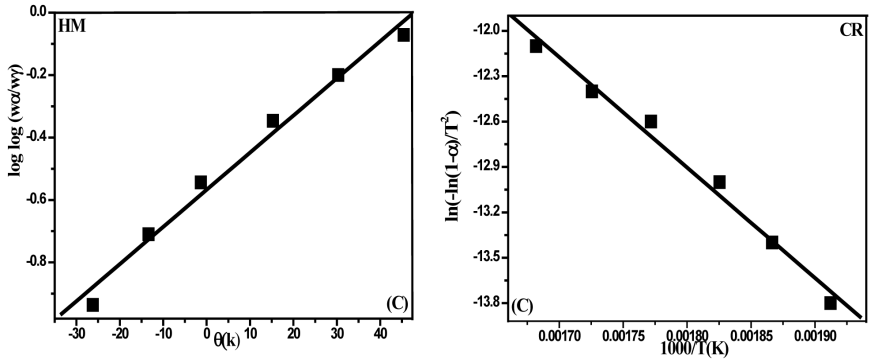

Figure S20. Kinetic data curves of: $[Cu_2MaTS(H_2O)_6]$ complex.

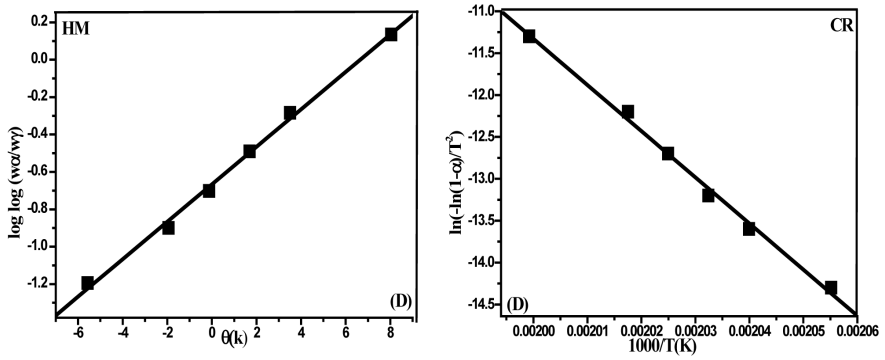

Figure S21. Kinetic data curves of $[Zn_2MaTS(H_2O)_6]$ complex.

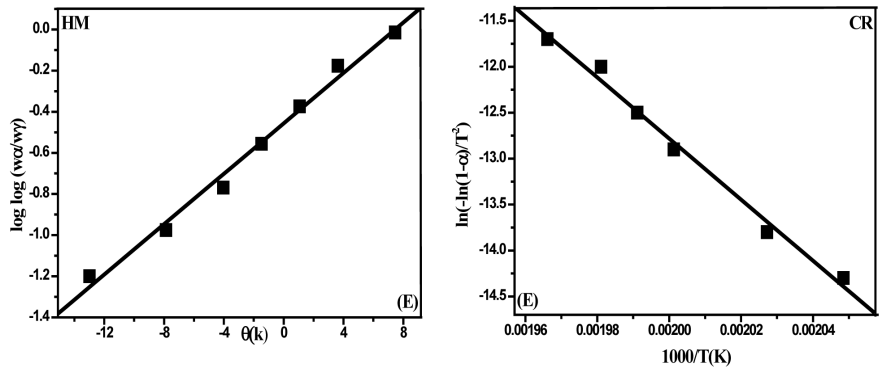

Figure S22. Kinetic data curves of $[Sn_2MaTS(H_2O)_6]\cdot 2H_2O$ complex.

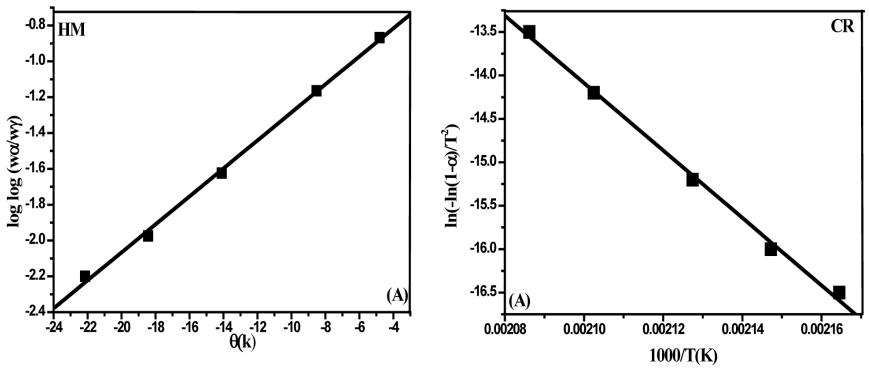

Figure S23. Kinetic data curves of 1,1-Succinyl-bis(4-phenyl thiosemicarbazide).

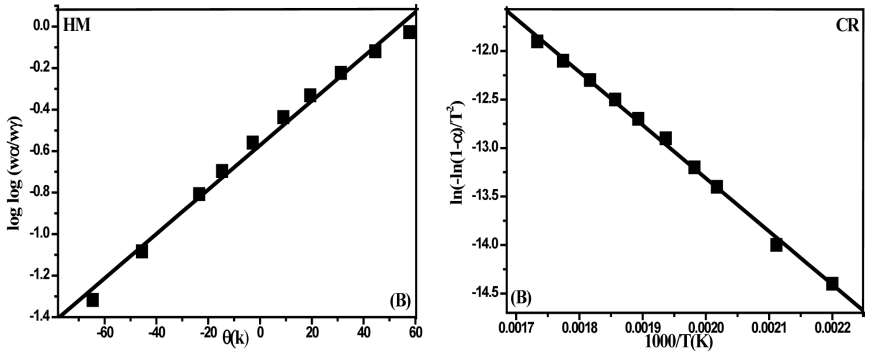

Figure S24. Kinetic data curves of $[Co_2SuTS(H_2O)_6]$ complex.

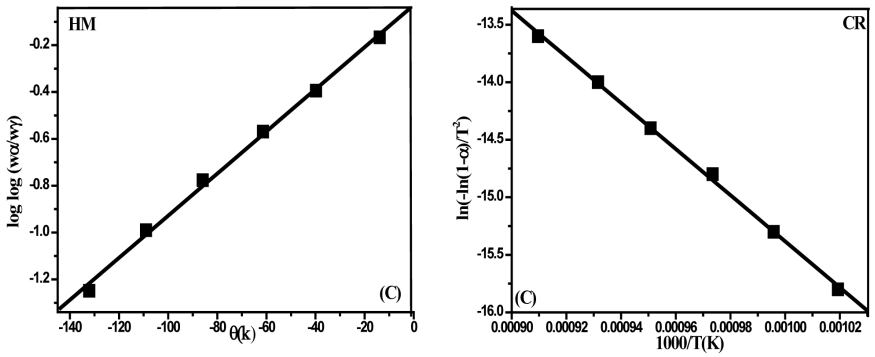

Figure S25. Kinetic data curves of $[Cu_2SuTS(H_2O)_6]$ complex.

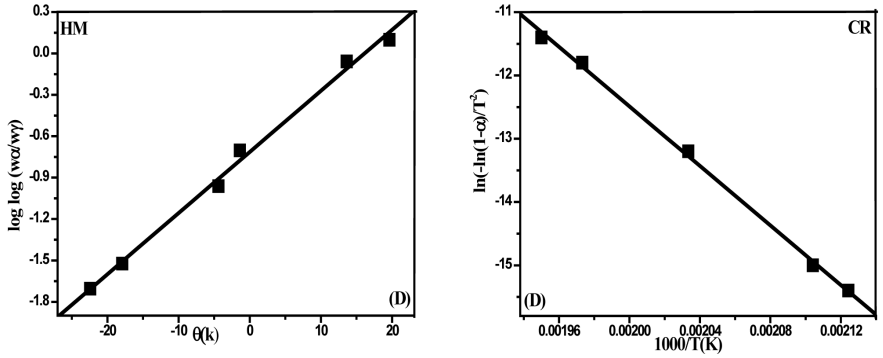

Figure S26. Kinetic data curves of $[Zn_2SuTS(ac)_2]\cdot 2H_2O$ complex.

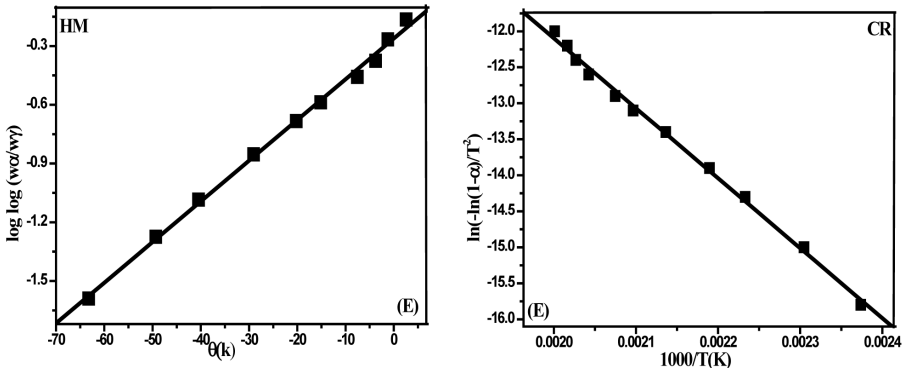

Figure S27. Kinetic data curves of $[Sn_2SuTS(H_2O)_6]$ complex.